Biochemical Characterization of *Thermocrispum agreste* TheA: A Flavin-Dependent N-hydroxylating Enzyme

Didier Philippe Mena-Aguilar

Thesis submitted to the faculty of

Virginia Polytechnic Institute and State University

in partial fulfillment of the requirements for the degree of

Master of Science

in

Biochemistry

Pablo Sobrado, Chair

Daniel J Slade

Bin Xu

May 07, 2018

Blacksburg, Virginia

Keywords: siderophores, flavoenzymes, hydroxylation, NADPH

Biochemical Characterization of *Thermocrispum agreste* TheA:

A Flavin-Dependent N-hydroxylating Enzyme

Didier Philippe Mena-Aguilar

ABSTRACT

N-hydroxylating monooxygenases (NMOs) are Class B flavin-dependent monooxygenases found only in fungi and bacteria. These enzymes catalyze the hydroxylation of nucleophilic primary amines, such as those found in histamine, L-ornithine, L-lysine, and small aliphatic diamines. The hydroxamate moiety produced by this reaction is key for the production of siderophores, small chelating compounds that allow survival in iron limiting conditions. NMOs involved in siderophore biosynthesis have been shown to be essential for pathogenesis in organisms such as *Aspergillus fumigatus*, *Pseudomonas aeruginosa*, and *Mycobacterium tuberculosis*. Therefore, NMOs are considered novel drug targets for the treatment associated with these diseases. Herein we present the characterization of TheA, an NMO from *Thermocrispum agreste*. The enzyme mechanism was studied using steady state kinetic measurements, thermostability, and stopped flow spectrophotometry assays. Using these techniques, the catalytic rates, substrate binding affinities, thermal stability, and coenzyme specificities were determined. Additionally, NADPH analogues were produced to use as tools to study FAD reduction in NMOs. An unspecific reduction reaction of $NADP^+$ using NaB^2H_4 yielded [6-^{2}H]-NADPH, [2-^{2}H]-NADPH, and [4-^{2}H]-NADPH. Compound identity was confirmed by mass spectrometry and unidimensional proton nuclear magnetic resonance (NMR). Results presented in this thesis lay the foundation for future studies of NMOs using NADPH analogues. In conjunction, these results will improve the general knowledge and understanding of flavoenzymes, ornithine monooxygenases, and their associated mechanisms.

Biochemical Characterization of *Thermocrispum agreste* TheA:

A Flavin-Dependent N-hydroxylating Enzyme

Didier Philippe Mena-Aguilar

GENERAL AUDIENCE ABSTRACT

Due to the surge of more potent and prevalent microbial pathogens, there is a constant search for new and more specific drugs. One approach is to identify and inhibit enzymes that are key for growth of these pathogens. An example of such enzymes is a group called N-hydroxylating monooxygenases (NMOs) that are key for the production of siderophores, small chelating compounds that allow survival of some fungi and bacteria in iron limiting conditions. NMOs involved in siderophore biosynthesis have been shown to be essential for pathogenesis in organisms such as Aspergillus fumigatus, Pseudomonas aeruginosa, and Mycobacterium tuberculosis. Therefore, NMOs are considered novel drug targets for the treatment associated with these diseases. To develop specific inhibitors of NMOs that can be used as drugs to treat these infections, we first need to understand how these enzymes work. Herein, we characterized a novel NMO from Thermocrispum agrestre. Our results highlight the similarities and differences from previously characterized NMOs. Furthermore, we produced analogues of NADPH, a molecule needed for the mechanism of NMOs. The produced compounds will be used in future studies to understand the step-by-step mechanism of the enzyme. In conjunction, these results will improve the general knowledge and understanding of NMOs and their associated mechanisms and lay the foundation for future studies on the identification of drugs that can be used to treat these diseases.

TABLE OF CONTENTS

LIST OF FIGURES

LIST OF TABLES

ACKNOWLEDGMENTS

First and foremost, I want to thank current and past members of the Sobrado Lab: my growth as a scientist and mentor is due to the constant support and encouragement they provided. I especially want to thank Dr. Julia S. Martin del Campo for training me in the first steps of my laboratory work. I would also like to extend my gratitude to Hannah Valentino for her friendship, advice, and teamwork. Working alongside Hannah has made my time in the Sobrado lab both more productive and fun! These motivating and beneficial experiences in the Sobrado Lab are attributed to the demanding but highly collaborative environment propitiated by Prof. Sobrado. For this reason, I extend my deepest gratitude to Prof. Pablo Sobrado for the opportunity to perform this research in his laboratory and for the expert mentorship and guidance I received.

I am grateful to my committee members Dr. Bin Xu and Dr. Daniel Slade for their time and advice in the development of my work. I would also like to thank Dr. Dirk Tishler and Marika Meinhert from Technische Universität Bergakademie Freiberg, Germany, for providing the plasmids used for protein expression in this work. I want to thank Dr. Yumin Dai for performing the NMR experiments and Keith Ray for performing the mass spectrometry experiments. I also thank Diane Eilerts and Jose Angel Rodriguez Corrales for providing invaluable advice on the writing of this thesis.

Finally, I want to thank my family and friends. Their constant love and support throughout my endeavors have inspired me to continue learning and growing in preparation for a successful future.

The research presented in this thesis was supported by grants from the National Science Foundation (NSF) CHE-1506206 and MCB-1021384 and funding from Consejo Nacional para Investigaciones Científicas y Tecnológicas de Costa Rica and Ministerio de Ciencia Tecnología y Telecomunicaciones de Costa Rica.

CHAPTER ONE: INTRODUCTION

I. Flavins and flavoenzymes

Flavoenzymes are proteins requiring a flavin cofactor, FMN or FAD, to perform a variety of physiologically significant functions in both catabolic and anabolic reaction pathways[1, 2]. The tricyclic isoalloxazine ring system of the flavin moiety offers kinetically and thermodynamically accessible redox states[3], which allows chemical intermediates to catalyze otherwise energetically unfavorable reactions (Figure 1.1). The ubiquitous presence of these enzymes across species, the diverse array of reactions they catalyze, and their potential applications in pharmaceutical, fine chemical and food industry, have rendered flavoenzymes a promising target of continuous research.

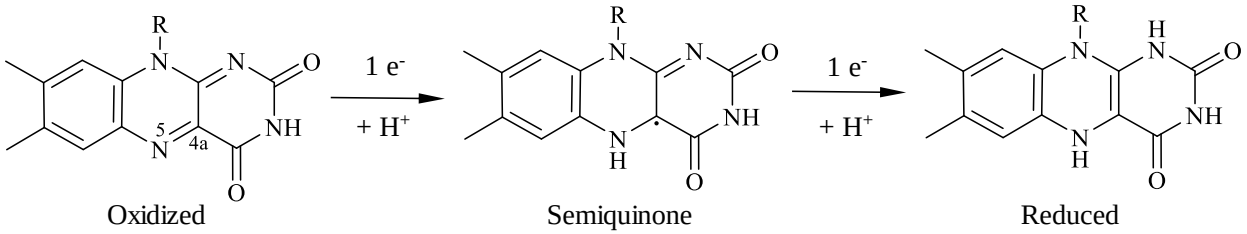

Figure 1.1 Redox states of flavin (only the isoalloxazine ring is shown).

While the reactions catalyzed by flavoenzymes are extremely diverse, these proteins share several conserved features. Flavoenzymes typically display high-affinity binding to the flavin via non-covalent interactions or, less commonly, covalent linkages. This high-affinity binding results in an extremely stable microenvironment in the active site, allowing for precise regulation of flavin reactivity[2]. The flavin binding site will vary depending on the specific flavin cofactor: those that bind FAD contain a Rossmann fold and those that bind FMN, a classic TIM barrel[4].

In general, flavoenzymes undergo a catalytic cycle consisting of two half reactions[3]. First, oxidized bound flavin is reduced by the incoming substrate in the reductive half reaction. Next, the flavin cofactor undergoes reoxidation to complete the subsequent oxidative half reaction[2].

The isoalloxazine ring contains two sites capable of undergoing covalent bond transformations. The N5 can undergo hydride additions and eliminations[5] as well as carbanion nucleophilic additions[6]. Additionally, the C4a can be covalently attached to thiols[7] or to oxygen adducts through the activation of molecular oxygen[8]. Flavoenzymes exploit the reactivity of these sites to facilitate reactions by stabilizing intermediates to decrease the activation energy of the reactions they catalyze.

II. Flavin-dependent monooxygenases

In flavin-dependent monooxygenases, the C(4a)-oxygen adducts act as stable intermediates to catalyze substrate oxidation in a wide range of biological processes (Figure 1.2). These enzymes incorporate one oxygen atom from the adduct into the substrate and reducing the other oxygen atom into water[9]. Flavin-dependent monooxygenases are the largest group of flavoenzymes that have been characterized[4] and are of particular interest due to their high enantio- and regio- selectivity[1].

Flavin-dependent monooxygenases are present in many biological processes, where they catalyze a number of reactions. Members of this group are known to catalyze hydroxylation, Baeyer-Villiger oxidation, sulfoxidation, epoxidation, oxidative decarboxylation, oxidative denitration, and halogenation reactions[9]. Flavin-dependent monooxygenases are further classified into eight groups, named A through H, based on fold and the reaction they catalyze. Groups A and B are encoded in a single gene and require NAD(P)H as an external electron donor. Groups C–F are two-component systems consisting of a flavin reductase that performs the first half reaction and a monooxygenase that uses reduced FAD or FMN to catalyze the second half reaction. Groups G and H comprise internal monooxygenases that reduce the flavin cofactor through substrate oxidation[9, 10].

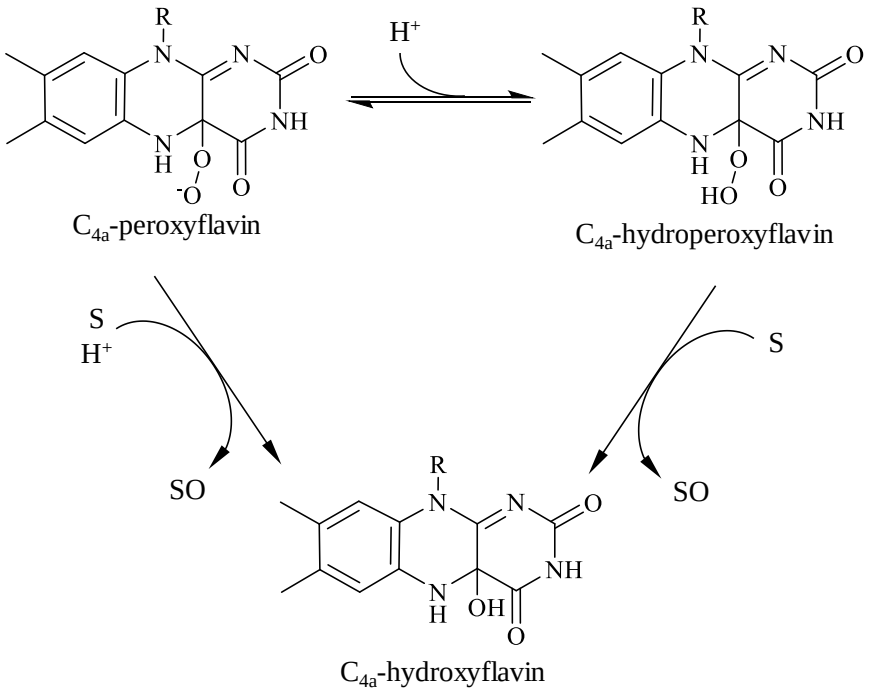

Figure 1.2 General mechanism of substrate oxygenation by flavin-dependent monooxygenases through C(4a)-oxygen adducts. S corresponds to the substrate.

Group B flavin-dependent monooxygenases are of particular interest due to their unique mechanism of action. In contrast to group A, group B enzymes do not require the substrate to initiate flavin reduction[11]. Furthermore, the nicotinamide cofactor remains bound to the enzyme even after the reduction step, forming a complex that plays key roles in the consecutive steps of the mechanism[12-15]. Group B flavin-dependent monooxygenases are encoded in a single gene and are composed of two Rossmann folds that bind FAD and NADPH. Based on sequence homology, four subgroups of group B have been described: Baeyer-Villiger monooxygenases, flavoprotein monooxygenases, N-hydroxylating monooxygenases (NMOs), and the YUCCA auxin biosynthesis enzymes[9, 11, 16, 17].

III. N-hydroxylating monooxygenases

NMOs are an example of Class B flavin-dependent monooxygenases that are only found in fungi and bacteria. These enzymes catalyze the hydroxylation of nucleophilic primary amines (Figure 1.3), such as those found in histamine, L-ornithine, L-lysine and small aliphatic diamines[10].

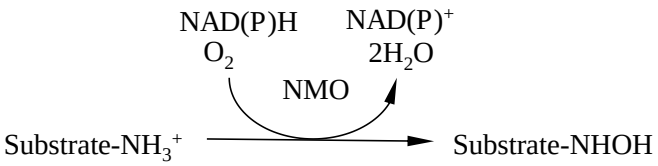

Figure 1.3. Reaction catalyzed by NMOs.

There is an evolutionary relationship between the structure and the substrate specificity of NMOs, as seen in the molecular phylogenetic tree analysis (Figure 1.4). Thus, the NMOs can be further classified depending on the substrate they act on. Several NMOs of each subgroup have been identified and characterized, with notable similarities and differences, both structurally and mechanistically, described for each group. L-ornithine monooxygenases are the most extensively studied group of NMOs; most notably, *Aspergillus fumigatus* SidA[13, 18-22] and *Pseudomonas aeruginosa* PvdA[23-26].

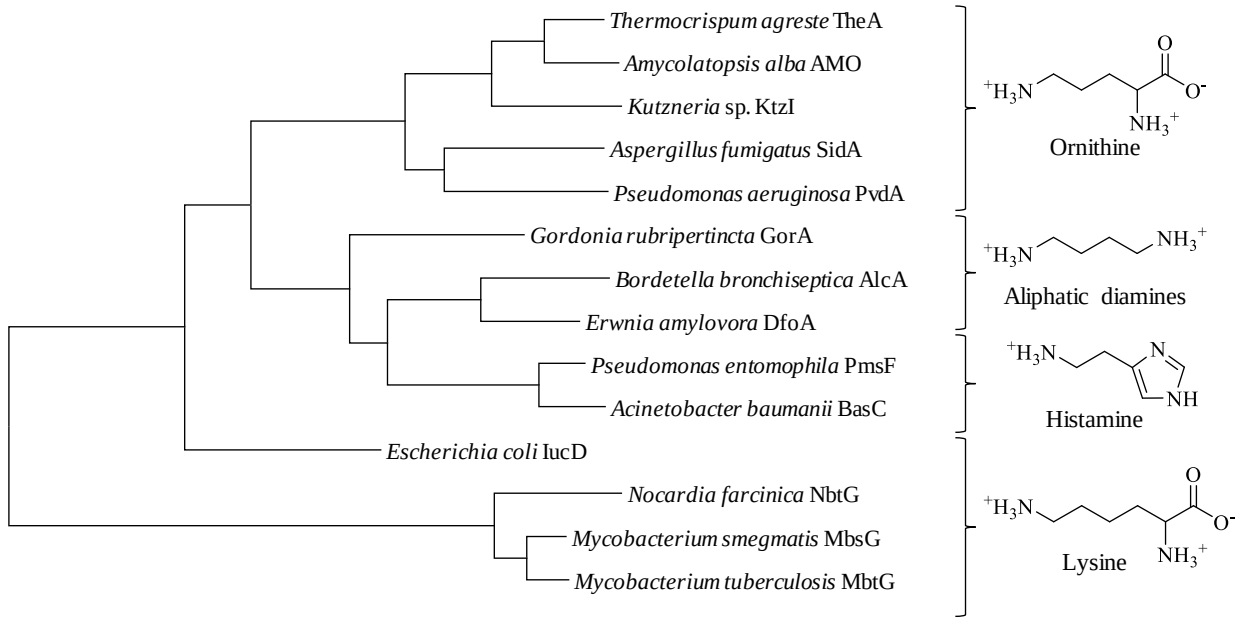

Figure 1.4 Molecular phylogenetic analysis of reported NMOs by Maximum Likelihood method as determined by MEGA7[27]. The substrate the enzymes hydroxylate is specified for each cluster.

The mechanism of L-ornithine monooxygenases (Figure 1.5) was elucidated by steady state kinetics[18, 23, 26], rapid reaction kinetic studies,[23, 28, 29] and density functional theory studies[30]. All NMOs reported to date follow the characteristic mechanism of flavin monooxygenases in which there is a reductive half reaction followed by an oxidative half reaction. After flavin reduction by NADPH, an oxygen activation step forms a C4a-hydroperoxyflavin intermediate. Consequently, substrate binding induces hemolytic cleavage of –OOH, forming two oxygen radicals. Transfer of the HO• radical occurs via a somersault rearrangement. Water released from C4a-hydroxyflavin catalyzes both the deprotonation and protonation steps to form the final product, N-hydroxy ornithine. Release of water and N-hydroxy ornithine finishes the reaction, regenerating free enzyme with oxidized flavin ready to start the reaction again[30].

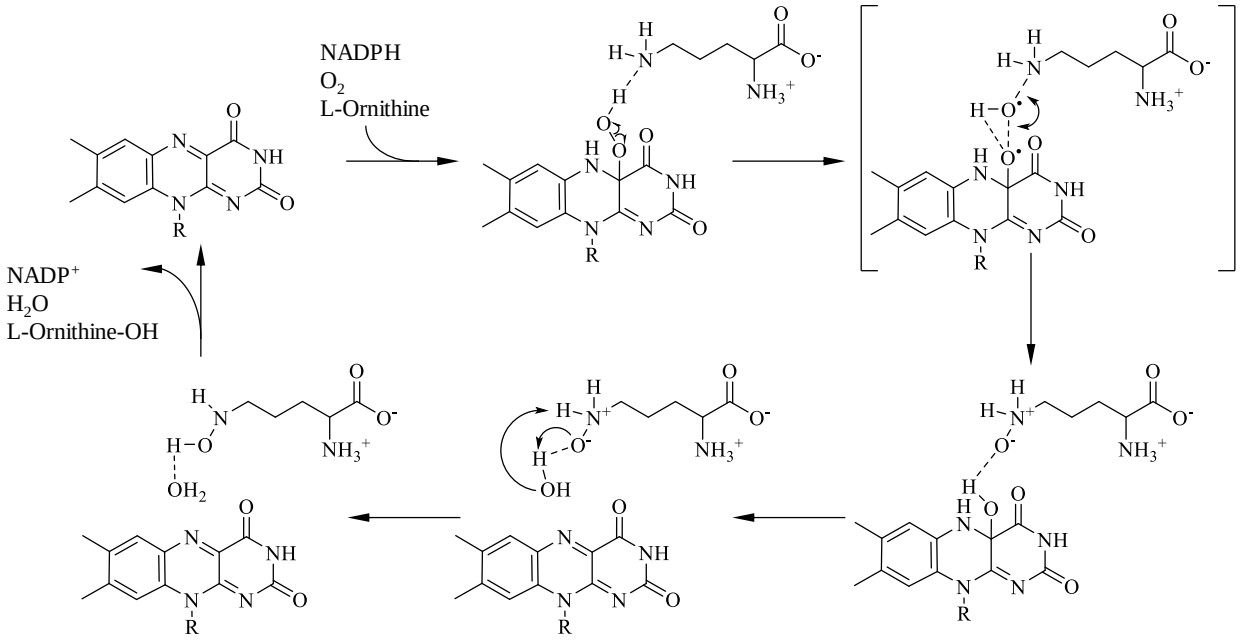

Figure 1.5 Proposed mechanism of the N-hydroxylation of L-ornithine by SidA[30]. After flavin reduction by NADPH and oxygen activation to form the C4a-hydroperoxyflavin intermediate. Binding of the substrate induces hemolytic cleavage of –OOH. Transfer of the HO• radical occurs via a somersault rearrangement. Water released from hydroxyflavin catalyzes the deprotonation/protonation steps to form the final N-hydroxy ornithine. The release of products finishes the reaction.

Determination of the PvdA[24] crystal structure provided the first structure of an NMO. Additional NMO crystal structures have since been reported, providing structural information of L-lysine[31] and diamine monooxygenases[32], as well as L-ornithine monooxygenases at different reaction steps[12, 33]. NMO structure consists of three domains: the FAD binding domain, NADPH binding domain, and substrate binding domain (Figure 1.6.A). In the active site, NADP(H) and ornithine form a ternary complex with FAD and the enzyme, setting up the spatial requirements for the reaction to occur (Figure 1.6.B).

Both the FAD and NADPH binding domains consist of a nucleotide-binding Rossmann fold with sequence motifs responsible for binding[34] that are conserved throughout NMOs[35]. However, the degree of solvent exposure of FAD varies significantly in each enzyme. This is reflected in the affinity for FAD and the ability to purify the enzymes with FAD bound. SidA binds FAD so that it is deeply buried in the domain[12]

and can be purified with FAD bound[18], whereas the PvdA binding cleft is shallow[24] and so it can only be purified without FAD bound[26]. Preference of the enzyme for NADPH over NADH is hypothesized to be dictated by the presence of two residues: Arg276 and Ser322 in SidA, which interact via hydrogen bonding with the phosphate group of the adenine ribose in NADPH[35].

L-Ornithine binds to NMOs in a small helical domain in which three key residues in SidA, Lys107, Asn293 and Ser469 (Figure 1.6.B), are responsible for interacting with the carboxylate and amino moieties of L-ornithine. These residues are conserved throughout all L-ornithine and L-lysine monooxygenases reported to date[24, 31, 33]. In the diamine aliphatic monooxygenase DfoA, however, these residues are replaced by the hydrophobic Ala60 and Leu238, which interact with the nonpolar aliphatic chain[32].

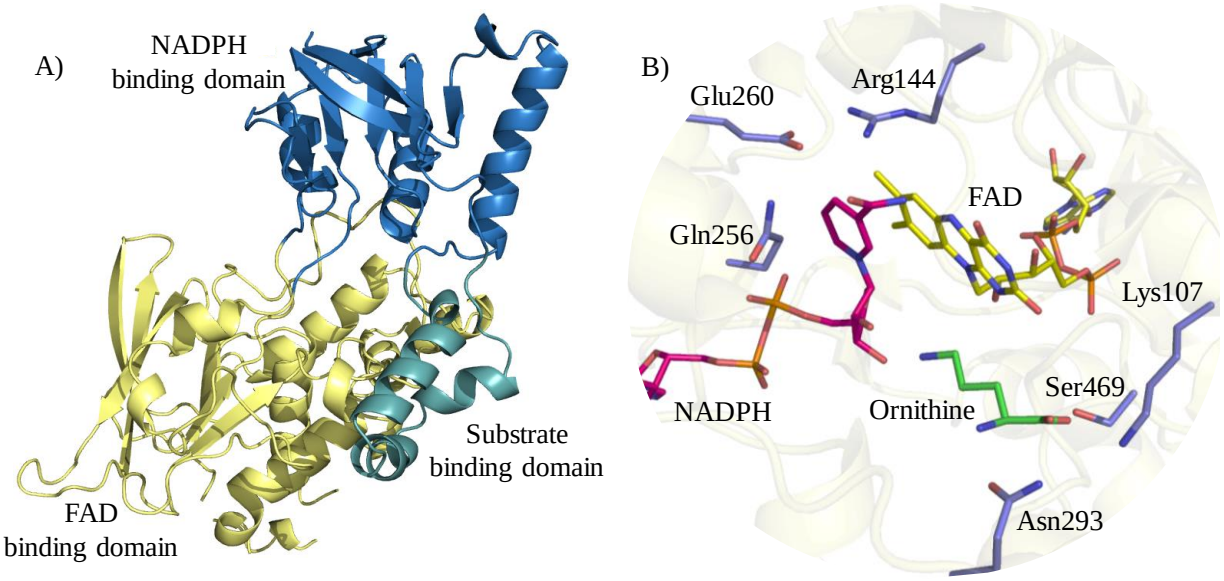

Figure 1.6 Structure of SidA, an L-ornithine NMO (PDB: 4B63)[12]. A) SidA is composed of a FAD binding domain, an NADPH binding domain, and a substrate binding domain, shown in yellow, blue, and green, respectively. B) SidA active site. FAD, NADPH, and ornithine are represented in yellow, pink, and green, respectively, and residues responsible for binding are shown in light blue.

IV. Biological role and significance of NMOs

NMOs are known to be involved in the production of antimicrobial compounds[36] and, most notably, siderophore biosynthesis[35]. Siderophores are low molecular weight compounds that chelate ferric ions. Siderophores are synthesized by fungi and bacteria as a response to iron starvation as they aid in scavenging iron and increasing iron availability[37]. NMOs are responsible for catalyzing the first step of siderophore biosynthetic pathways. Hydroxylation of substrate amino group by NMOs yields a hydroxamate moiety that is directly responsible for binding ferric ions in siderophores (Figure 1.7).

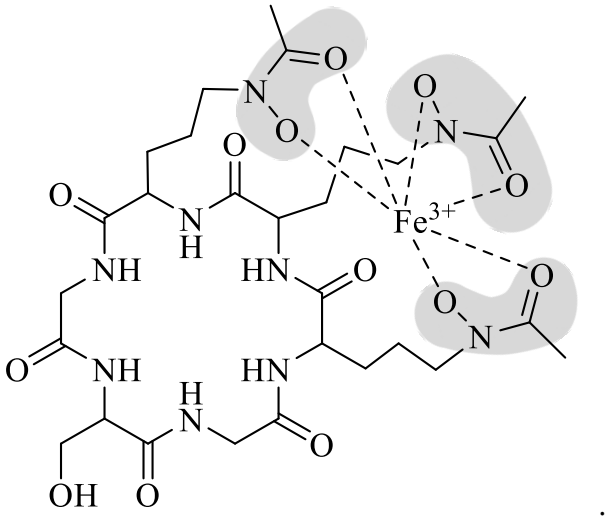

Figure 1.7 Ferrichrome, a siderophore from *A. fumigatus*. The hydroxamate moieties responsible for interacting with the ferric ion are highlighted in gray.

Siderophore biosynthesis and the NMOs involved in siderophore biosynthesis have been shown to be essential for pathogenesis in organisms such as *A. fumigatus*[38], *P. aeruginosa*[39], and *M. tuberculosis*[40]. Therefore, NMOs show great potential as novel drug targets that can be used to treat associated diseases. Initial studies have been reported, in which through high throughput screening, an inhibitor of SidA was identified and validated. Furthermore, this compound was shown to inhibit *A. fumigatus* growth by blocking the siderophore biosynthesis pathway through SidA inhibition[41].

Due to their unique mechanism and potential as drug targets, NMOs remain relevant as the objective of continuous research. In this study, we biochemically characterized a novel L-ornithine monooxygenase from *Thermocrispum agreste*. We proposed to use this enzyme as a model NMO to obtain novel insights that will help us better understand the behavior and mechanism of flavoenzymes and L-ornithine monooxygenases. Furthermore, we produced and purified NADPH analogues that we propose to use as probes to study the reduction of flavin in the NMOs mechanism.

CHAPTER TWO: ENZYMATIC CHARACTERIZATION OF *Thermocrispum agreste* TheA: A FLAVIN-DEPENDENT N-HYDROXYLATING ENZYME

I. Introduction

NMOs are enzymes that catalyze the hydroxylation of amino groups in a diverse range of small molecules[10, 35]. A group of these enzymes is characterized for hydroxylating L-ornithine in biosynthetic pathways that are known to produce metabolites involved in siderophore[19, 42] and antimicrobial compound[36] biosynthesis. Structural and mechanistic characterization of such enzymes has been previously reported; most notably *Aspergillus fumigatus* SidA[12, 18, 20, 30, 43], *Pseudomonas aeruginosa* PvdA[24, 26], and *Kutzneria* sp. KtzI[33, 36].

Previous bioinformatic studies[44] have resulted in the identification of a putative siderophore synthesis gene cluster in the genome of *Thermocrispum agreste* (Accession: WP_028847741.1), a thermostable actinomycete capable of growing in temperatures ranging from 28 °C to 60 °C[45]. The structure of the *T. agreste* siderophore Thermochelin (Figure 2.1) was predicted by similarity search and annotation of the gene cluster, which is comprised of amino acid modifying enzymes, transporters, and regulators[44].

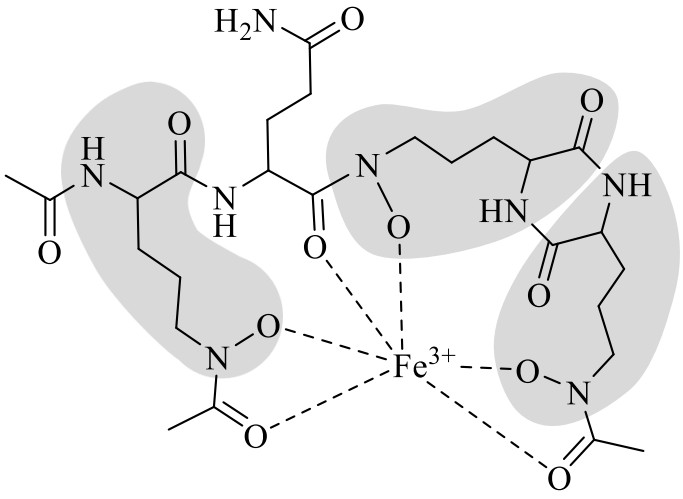

Figure 2.1 Proposed structure of *T. agreste* siderophore, Thermochelin[44]. Atoms derived from ornithine are shaded in gray.

The *T. agreste* L-ornithine monooxygenase, referred from now on as TheA, was bioinformatically and experimentally identified as the enzyme responsible for the production of Thermochelin hydroxamate moieties (Figure 2.2)[44]. Phylogenetic analyses have shown that TheA is evolutionary closely related to ornithine monooxygenases from other actinomycetes (Figure 1.4). Specifically, TheA has 62.64% sequence identity with *Amycolapsis alba* AMO and 49.88% sequence identity with *Kutzneria* sp KtzI, as determined via multiple sequence alignment[46].

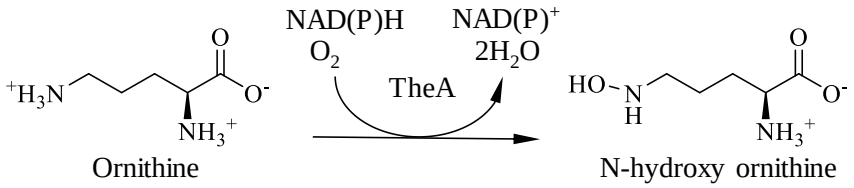

Figure 2.2 N-hydroxylation of L-ornithine by TheA. The enzyme uses NADPH and O_2 as cosubstrates to catalyze the production N-hydroxy ornithine.

In this chapter, the expression, purification, and initial biochemical characterization of TheA are presented. Steady state kinetics were determined by following the rate of both oxygen consumption and product formation. This information was used to experimentally determine the substrate and cosubstrate specificity as well as steady state rate constants. Furthermore, we determined physical properties of the enzyme including the melting temperature and thermal stability. Finally, by performing presteady state kinetics, we determined the rate constant of flavin reduction on the reductive half reaction. In conjunction, these results will advance our knowledge and understanding of flavoenzymes, ornithine monooxygenases, and their associated mechanisms.

II. Material and methods

2.2.1 Materials

The DNA encoding the *T. agreste* TheA gene ligated into the pET16b plasmid was kindly provided by Dr. Dirk Tischler from Technische Universität Bergakademie Freiberg in Germany. Reagents used in this work were obtained from Fisher Scientific (Pittsburg, PA) unless otherwise stated.

2.2.2 Heterologous Expression and Purification of TheA

The pET16b plasmid encoding for TheA was transformed into Turbo BL21 (DE3) *Escherichia coli* cells (Sigma Chemical Co.) and successful transformants were selected by growing the cell overnight at 37 °C in agar plates containing 100μg/ml of ampicillin[47]. A seed culture was prepared by inoculating 100 mL of Luria-Bertani (LB) media with a transformed colony and incubating overnight (~16 h) at 37 °C. The seed culture was used to inoculate 6 L of Terrific Broth autoinduction media. The cultures were incubated at 37 °C with shaking (250 rpm) to a final optical density at 600 nm of 4, at which time the incubation temperature was lowered to 18 °C. This procedure typically yielded ~24 g of cells per liter of culture media. The cell pellet was frozen and stored at -80 °C until purification.

For protein purification, the cell paste was resuspended at a ratio of 1 gram of cells per 5 mL of Buffer A (25 mM HEPES, 300 mM NaCl, 25 mM imidazole, pH 7.5) and incubated with 60 μg/mL of lysozyme, and 20 μg/mL each of DNAse I, and RNAse for 30 min at 4 °C with constant stirring. The resulting cell suspension was lysed by sonication at 70% amplitude for a total of 5 min using a pulsing (5 s on, 10 s off) ultrasonic probe. During sonication, the suspension was incubated on ice. The lysate was centrifuged at 45,000 g for 45 min at 4 °C. The supernatant was then collected and loaded onto two tandem 5 mL HisTrap columns previously equilibrated with Buffer A. After loading of the supernatant, the columns were washed with Buffer A until absorbance at 280 nm returned to baseline level. The columns were then washed with Buffer B (25 mM HEPES, 300 mM NaCl, 50 mM imidazole, pH 7.5). TheA was eluted with Buffer C (25 mM HEPES, 300 mM NaCl, 300 mM imidazole, pH 7.5). Eluent fractions containing purified protein were

pooled and buffer exchanged by dialysis into storage buffer (25 mM HEPES and 100 mM NaCl, pH 7.5). The enzyme solution was then concentrated to 100 μM, flash frozen in liquid nitrogen, and stored at -80 ºC. Protein concentration was determined using the Bradford Assay and fractions obtained throughout the process were analyzed with an SDS-PAGE.

2.2.3 Determination of the Extinction Coefficient

The absorbance spectrum of TheA (45 μM) was determined in a 1-cm pathlength quartz cuvette in a UV/Vis spectrophotometer (Agilent, Santa Clara, CA). After recording the spectrum, the sample was removed and incubated at 95 °C for 1 min. The denatured solution was then centrifuged at 5000 rpm for 5 min and the amount of FAD in the supernatant was determined. An extinction coefficient at 450 nm of 11.06 mM^{-1} cm^{-1} was calculated for TheA from the known extinction coefficient of free FAD (ε_{450}: 11.3 mM^{-1} cm^{-1}).

2.2.4 Gel Filtration Chromatography

TheA (0.15 mM) was loaded onto a HiPrep Sephacryl S-200 HR column (GE Healthcare) equilibrated with buffer containing 50 mM potassium phosphate and 0.15 mM NaCl at pH 7.5. Ribonuclease A (13700 Da), ovalbumin (43000 Da), conalbumin (75000 Da), aldolase (158000 Da), Blue Dextran200 (200000 Da), and Ferritin (440000) were used as standards to determine the molecular mass of TheA in solution.

2.2.5 Oxygen Consumption Assay

The amount of molecular oxygen consumed by TheA was monitored using an Oxygraph (Hansatech, Norfolk, England). The standard assay consisted of 100 mM sodium phosphate, pH 7.5. TheA (2.5 μM) was incubated in buffer at 25 °C before the reaction was initiated by the addition of substrates. The reaction proceeded for 1 min at 25 °C with constant stirring.

2.2.6 Product Formation Assay

The amount of hydroxylated product formed by TheA was assayed by a variation of the Csaky iodine oxidation test[48] modified as previously described[18]. The standard assay buffer contained 100 µL of 100 mM potassium phosphate buffer at pH 7.5 and varying concentrations of L-ornithine or L-lysine and NADPH or NADH. TheA (2.5 µM) was incubated in the assay buffer at 25 °C before the reaction was initiated by the addition of the NAD(P)H. The reaction proceeded for 15 min at 25 °C with shaking and was terminated by the addition of perchloric acid. The absorbance at 562 nm was measured after 15 min on a SpectraMax M5e plate reader (Molecular Devices, Sunnyvale, CA). A hydroxylamine hydrochloride standard curve was used to calculate the amount of hydroxylated product produced.

2.2.7 Thermal Stability

To determine the thermal stability of the protein, TheA (2.5 µM) was incubated for 10 minutes at 10, 20, 30, 40, 50, and 60 °C in 100 mM sodium phosphate, pH 7.5. The protein was allowed to cool to room temperature before determining the activity. The reaction was initiated by adding 2 mM L-ornithine and 2 mM NADPH and incubating with agitation for 15 min at room temperature. The effect on enzyme activity was determined by measuring product formation via the iodine oxidation assay and calculating the percent decrease in activity.

2.2.8 ThermoFAD assay

The melting temperature (T_m) of the protein was determined by the ThermoFAD assay[49], in which 50 µL of 3 mg/mL TheA in 100 mM Sodium Phosphate buffer at pH 7.5 was exposed to heat, increasing the temperature 20–90 °C in 1 °C increments. The T_m of TheA was determined in the absence and in the presence of 15 mM L-ornithine and 1 mM $NADP^+$. FAD fluorescence was measured using an excitation wavelength range between 470 and 500 nm and a SYBR Green fluorescence emission filter of 523–543 nm. The melting temperature was determined by calculating the inflection point of the fluorescence as a function of temperature.

2.2.8 Flavin reduction presteady state kinetics

Reduction of FAD bound to TheA was monitored using stopped flow spectrometry (Applied Photophysics SX20, Leatherhead, UK) under anaerobic conditions, as previously described[50]. Flavin reduction was monitored with a photodiode array spectrometer until full reduction of FAD was achieved, which was detected by a decrease in absorbance at 450 nm. Measurements were obtained in triplicate and recorded on a logarithmic scale. Reaction buffer consisted of anaerobic 100 mM sodium phosphate buffer at pH 7.5. The reaction mixture consisted of 20 μM enzyme and 0.01–2 mM NADPH. Experiments were performed both in the absence and presence of 10 mM L-ornithine.

2.2.9 Data Analysis

Kinetic data was analyzed using the programs KaleidaGraph (Synergy, Reading, PA). Initial rate data was fit to the Michaelis-Menten equation to obtain k_{cat} and K_M values (Equation 1). For the reductive half reaction, the decrease in absorbance at 450 nm was fitted to a double exponential decay equation to obtain the k_{obs1} and k_{obs2} of the reduction process at a specific NADPH concentration (Equation 2). The resulting k_{obs1} and k_{obs2} were plotted as a function of NADPH, and the data was fitted to Equation 3 to obtain k_{red} and K_D.

$$v/[E] = \frac{k_{cat}[S]}{K_M + [S]} \qquad \text{Equation 1}$$

$$v = a_1 e^{(-k_{obs1} \times t)} + a_2 e^{(-k_{obs2} \times t)} + c \qquad \text{Equation 2}$$

$$k_{obs} = \frac{k_{red}[S]}{K_D + [S]} \qquad \text{Equation 3}$$

III. Results

2.3.1 Expression and purification of TheA

Recombinant TheA was expressed in Turbo BL21 (DE3) *Escherichia coli* cells as an N-terminal His•Tag® fusion protein. The incorporation of the His-tag allowed the protein to be purified using immobilized nickel affinity chromatography. After purification, approximately 60% of the expressed recombinant protein was found insoluble in the pelleted fraction (Figure 2.3.A). Soluble TheA was eluted from the column with 300 mM imidazole. A standard purification yielded 2.4 mg of protein per gram of cell paste. TheA displayed an absorbance spectrum consistent with a flavoprotein (Figure 2.3.B) and the extinction coefficient at 450 nm was determined to be 11.06 mM^{-1} cm^{-1}. The FAD-bound purified protein fraction of the purified protein comprised approximately 68% of the total protein, as determined by the Bradford Assay.

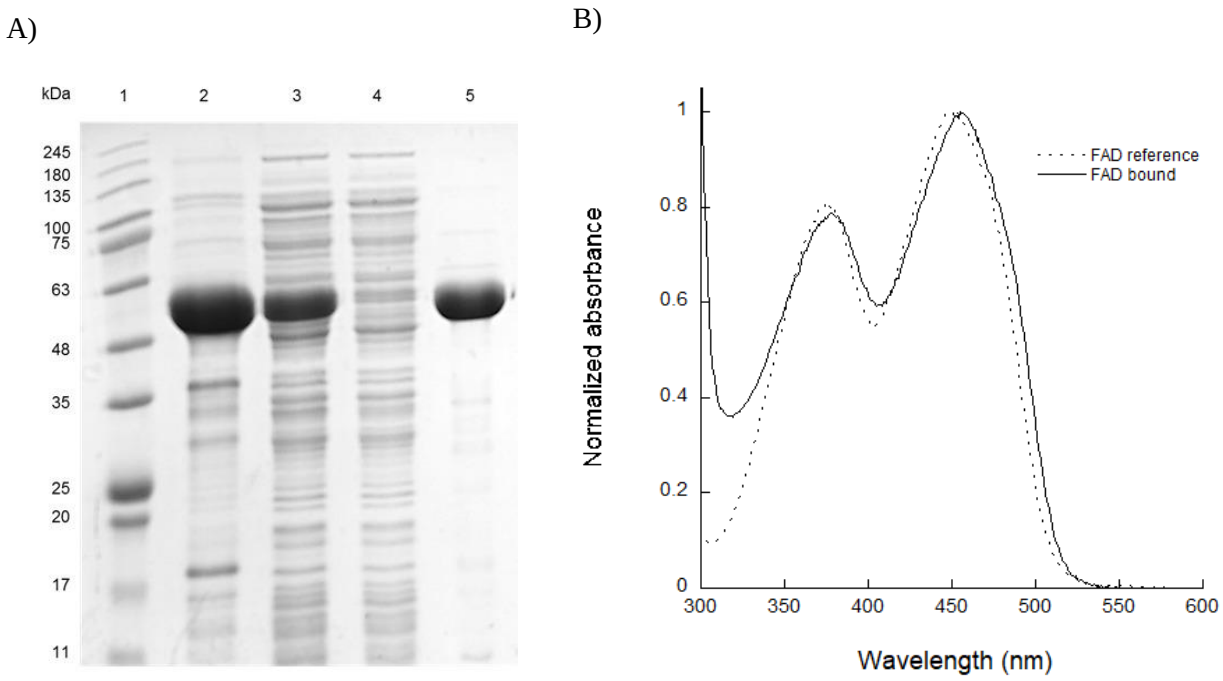

Figure 2.3 Purification summary of TheA (A) SDS-PAGE gel 1. Molecular weight ladder, 2. Pellet, 3. Supernatant, 4. Flow through, 5. Elution 300 mM imidazole. (B) UV-visible spectrophotometry of bound FAD.

The molecular weight of TheA is 51.5 kDa (Table 2.1), as determined *in silico* using the ProtParam tool (Expasy) and confirmed experimentally by SDS-PAGE analysis (Figure 2.3.A). Size-exclusion chromatography results (Figure 2.4) suggest that TheA exists in solution primarily in an octameric state and, to a lesser degree, in a pentameric state (Table 2.1).

Table 2.1 Solution molecular weight of TheA.

Peak	Experimental MW (kDa)	Calculated MW(kDa)	Multimeric State
1	235.6	51.5	Pentameric
2	390.2		Octameric

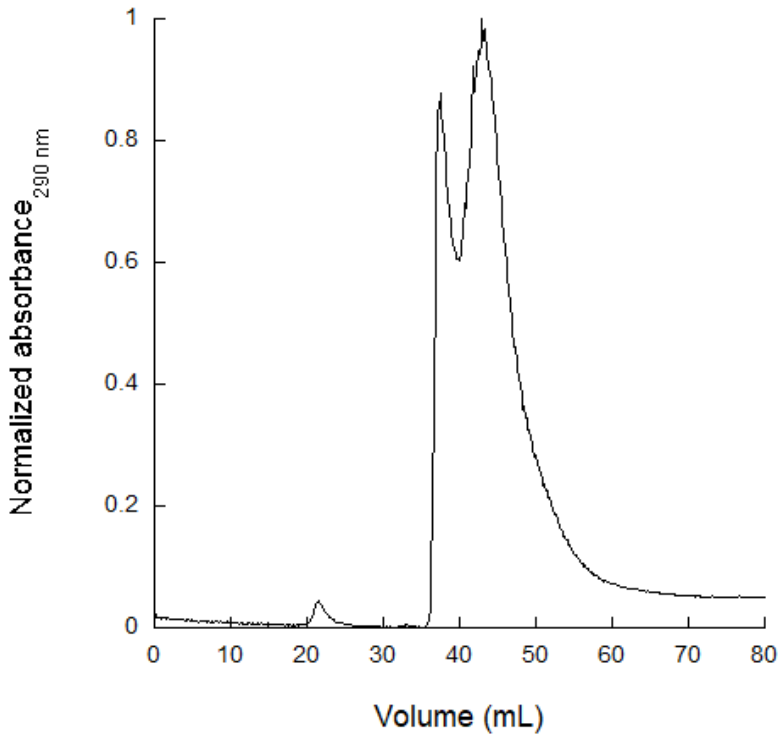

Figure 2.4 Size exclusion chromatogram of TheA.

2.3.2 Steady state kinetic characterization of TheA

Steady state kinetic parameters of TheA determined using the oxygen consumption and product formation are summarized in Table 2.2 and Table 2.3, respectively. Substrate saturation curves were determined by monitoring the initial enzyme rate at increasing concentrations of L-ornithine or L-lysine. When provided L-ornithine as the substrate (Figure 2.5.A), TheA consumed oxygen with a k_{cat} of 0.128 ± 0.004 s^{-1} and a K_M of 0.048 ± 0.008 mM. TheA hydroxylated L-ornithine with a k_{cat} of 0.11 ± 0.01 s^{-1} and K_M of 0.37 ± 0.09 mM. In contrast, when provided L-lysine as the substrate, the purified recombinant enzyme consumed oxygen with a k_{cat} of 0.050 ± 0.003 s^{-1} and K_M of 0.005 ± 0.003 mM, and, interestingly, no product was detected when using the product formation assay (Figure 2.5.B). Nicotinamide cofactor saturation curves were determined by monitoring the initial enzyme rate of at increasing concentrations of NADPH or NADH. When using NADPH as the cofactor (Figure 2.5.C), TheA consumed oxygen with a k_{cat} of 0.171 ± 0.005 s^{-1} and K_M of 0.050 ± 0.003 mM. The enzyme hydroxylated L-ornithine with a k_{cat} of 0.104 ± 0.009 s^{-1} and K_M of 0.18 ± 0.05 mM. When using NADH as the cofactor (Figure 2.5.D), the enzyme consumed oxygen with a k_{cat} of 0.120 ± 0.006 s^{-1} and K_M of 0.56 ± 0.09 mM, and hydroxylated L-ornithine with a k_{cat} of 0.036 ± 0.004 s^{-1} and K_M of 1.0 ± 0.2 mM.

By comparing the turnover number obtained by monitoring oxygen consumption and the product formation assay, the percent uncoupling can be determined. When using L-lysine as the cofactor, no product was detected, suggesting complete (100%) uncoupling. Alternatively, when L-ornithine is provided as the substrate, 39% uncoupling is observed with NADPH as the cofactor and 70% with NADH as the cofactor (Table 2.4).

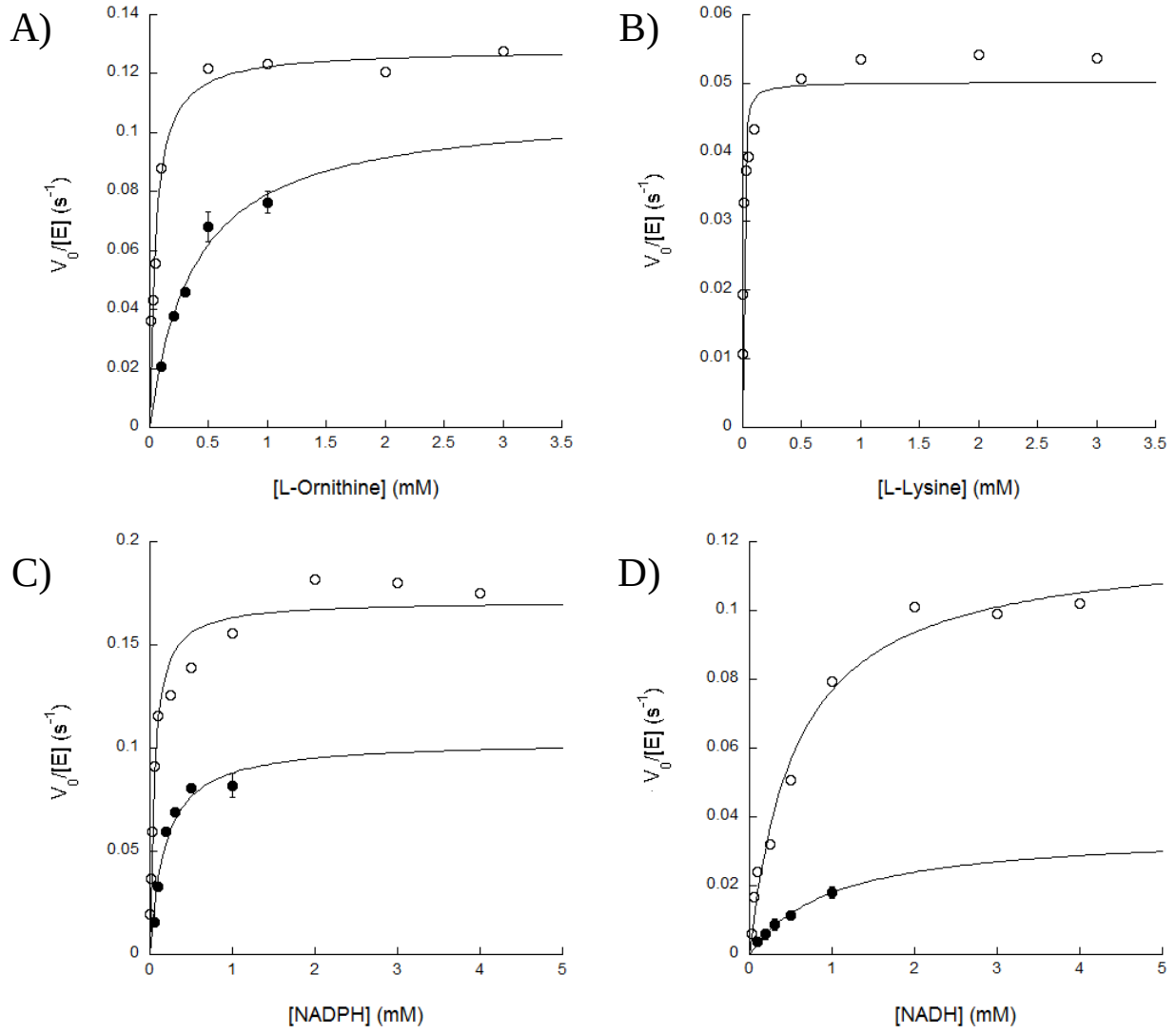

Figure 2.5 Ornithine (A), lysine (B), NADPH (C) and NADH (D) saturation curves as determined by the product formation (●) and oxygen consumption assays (○). Enzymatic reactions were performed at room temperature for 15 minutes in 100 mM sodium phosphate buffer. 2 mM NADPH was used when varying substrate concentrations and 2 mM L-Ornithine was used when varying reduced nicotinamide coenzyme concentrations.

Table 2.2 Steady state kinetic parameters of TheA, oxygen consumption.

Substrate	k_{cat} (s^{-1})	K_M (mM)	k_{cat}/K_M (s^{-1} mM^{-1})
L-ornithine	0.128±0.004	0.048±0.008	2.7±0.4
L-lysine	0.050±0.003	0.005±0.003	10±6
NADPH	0.171±0.005	0.050±0.009	3.4±0.6
NADH	0.120±0.006	0.56±0.09	0.21±0.04

Table 2.3 Steady state kinetic parameters of TheA, product formation.

Substrate	k_{cat} (s^{-1})	K_M (mM)	k_{cat}/K_M (s^{-1} mM^{-1})
L-ornithine	0.11±0.01	0.37±0.09	0.30±0.08
L-lysine	No product detected		
NADPH	0.104±0.009	0.18±0.05	0.6±0.2
NADH	0.036±0.004	1.0±0.2	0.036±0.008

Table 2.4 Uncoupling.

Reduced Nicotinamide Cofactor	Uncoupling (%)
NADPH	39
NADH	70

2.3.3 Temperature effect on TheA activity

TheA thermal stability was determined by incubating the enzyme at varying temperatures and calculating the activity via the product formation assay. TheA maintained activity close to 100% when incubating the enzyme at temperatures ranging from 10 °C to 50 °C and abruptly decreased below detectable levels when incubating at 60 °C (Figure 2.6).

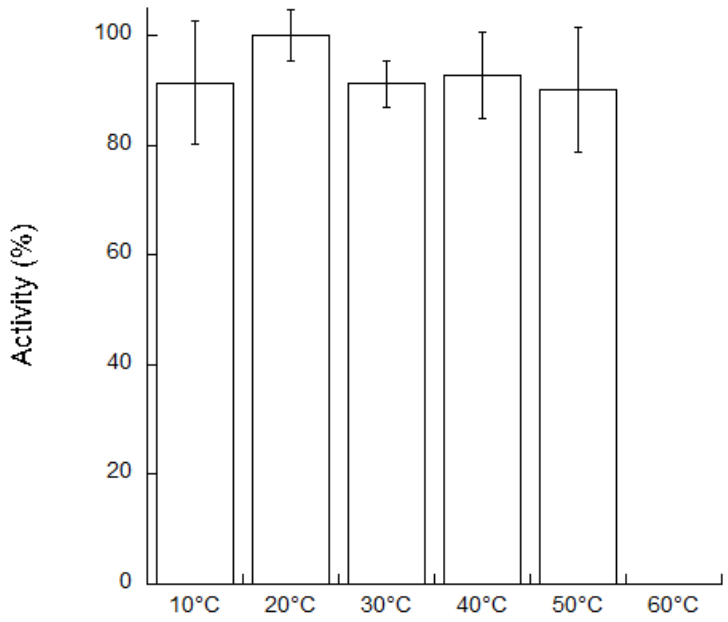

Figure 2.6 Thermostability of TheA.

The melting temperatures of TheA in the absence and in the presence of 15 mM L-ornithine and 1 mM $NADP^+$ was determined by calculating the inflection point of the curve obtained when monitoring the FAD fluorescence as a function of increasing temperature (Figure 2.7). In the absence of substrates, TheA had a T_m of 42.7 ± 0.1 °C and in the presence of substrates, TheA had a T_m of 50.1 ± 0.1 °C.

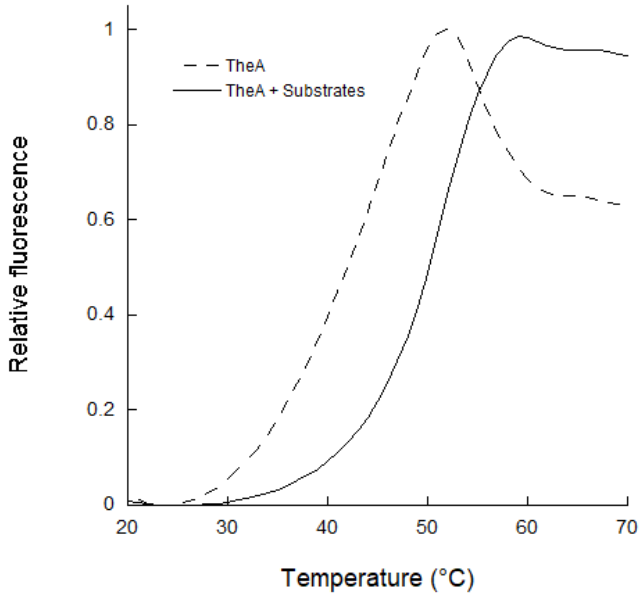

Figure 2.7 ThermoFAD assay to determine the melting temperature of TheA. The assay was performed in the absence and presence of 1 mM $NADP^+$ and 15 mM L-Ornithine.

2.3.4 Presteady state kinetic characterization of TheA

Flavin reduction was monitored as a function of NADPH both in the presence and absence of L-ornithine. The reaction was monitored by the decrease in absorbance at 450 nm (Figure 2.8.A and Figure 2.8.B) in the stopped flow spectrophotometer using single-mixing mode. FAD reduction was dependent on NADPH concentration, with increasing rates at higher NADPH concentration (Figure 2.8.C and Figure 2.8.D).

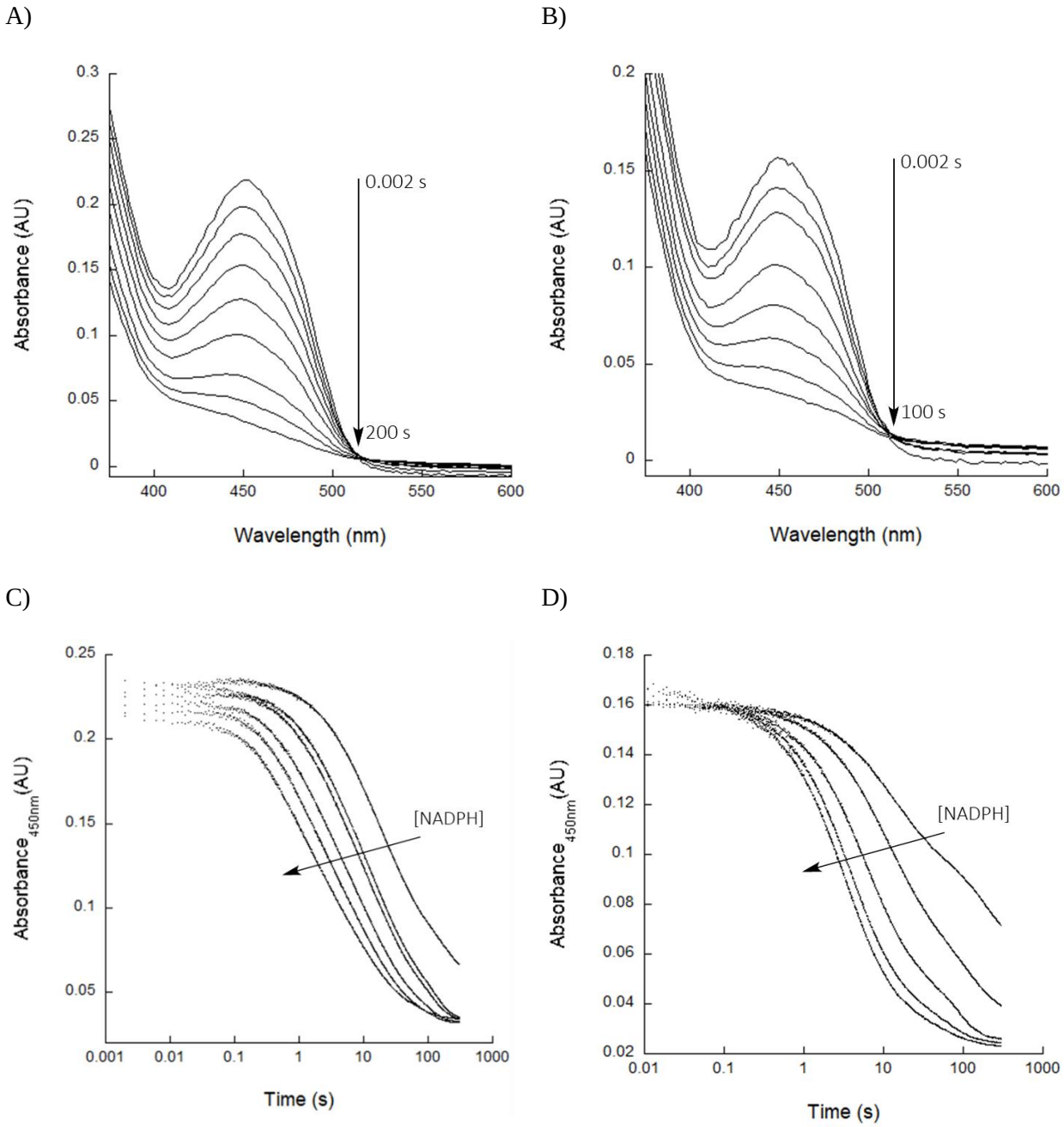

Figure 2.8 Reductive half reaction of TheA with NADPH. Time resolved absorption spectra of TheA in the presence of 25 μM NADPH and A) without or B) with 10 mM L-ornithine. Reduction of the absorbance at 450 nm of TheA at different concentrations of NADPH C) without or D) with 10 mM L-ornithine.

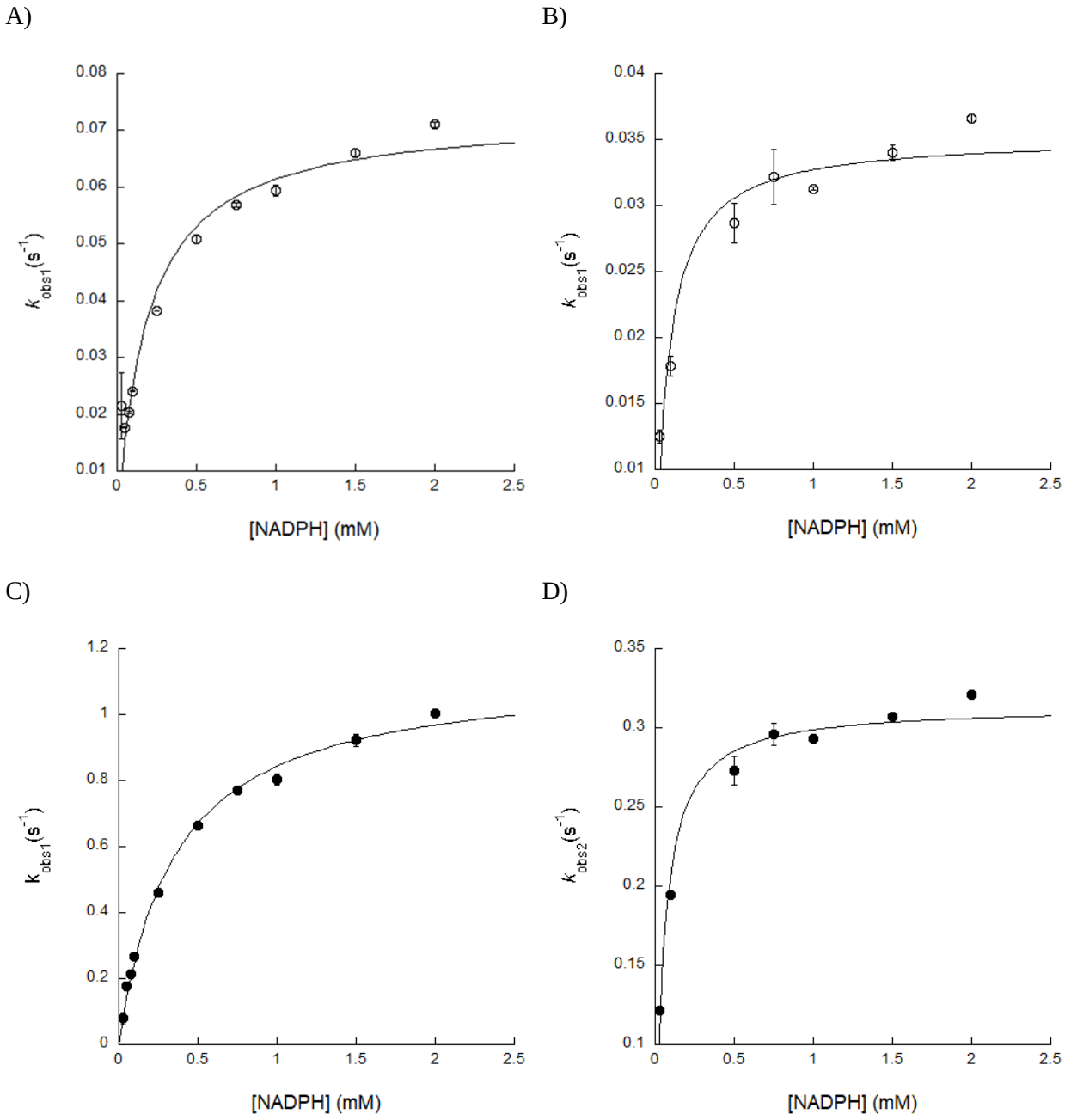

Figure 2.9 Presteady state kinetics of the reductive half reaction. The absorbance changes at 450nm were fit to Equation 2. The k_{obs1} values measured at each concentration of NADPH and plot as a function of NADPH concentrations in the absence (A) and presence (B) of 10 mM L-ornithine. The k_{obs2} in the absence (C) and presence (D) of 10 mM L-ornithine was fitted as well.

Reduction of the absorbance at 450 nm was fitted to a double exponential equation to solve for k_{obs1} and $k_{obs2,}$ which were plotted independently as a function of NADPH (Figure 2.9). The presteady state kinetic parameters of the TheA reductive half reaction were calculated by fitting k_{obs} as a function of NADPH concentration plots to Equation 3 (Table 2.5). In the absence of L-ornithine, k_{obs1} described a slower reaction with k_{red} of 0.073 ± 0.004 s^{-1} and K_D of 0.19 ± 0.04 mM, while the k_{obs2} described a fast reaction of k_{red} of 1.14 ± 0.03 s^{-1} and K_D of 0.35 ± 0.03 mM. The catalytic efficiency (k_{red}/K_D) for the fast reaction was higher than that of the slow reaction, where 3.3 ± 0.3 s^{-1} mM^{-1} and 0.38 ± 0.08 s^{-1} mM^{-1} were calculated for each respective reaction.

The reduction kinetics of TheA in the presence of ornithine produced results similar to those when no substrate was present in the reaction. The reduction was also fitted to a double exponential equation that produced kinetic parameters for two distinct phases. The slow phase, described by the k_{obs1}, produced a k_{red} of 0.035 ± 0.002 s^{-1} and K_D of 0.08 ± 0.02 mM. The k_{obs2} described a fast reaction of k_{red} of 0.314 ± 0.007 s^{-1} and K_D of 0.050 ± 0.008 mM. The catalytic efficiency k_{red}/K_D for the fast reaction was also higher than that of the slow reaction, where 6 ± 1 s^{-1} mM^{-1} and 0.4 ± 0.1 s^{-1} mM^{-1} were calculated for each reaction, respectively.

Interestingly, the reductive reaction yielded a k_{red} ~3.5 fold higher in the absence of the substrate than in the presence of substrate for the fast phase and ~2 fold higher for the slow phase. On the other hand, the K_D for both the fast and slow phases were ~7 and ~2 fold lower in the presence of substrate. The enzyme in the presence of the substrate seems to be twice as efficient in the fast phase and remained the same in the slow phase, as evidenced by the changes in the $k_{red}/K_{D.}$

Table 2.5 Presteady state kinetic parameters of TheA reductive half reaction.

	Phase	k_{red} (s^{-1})	K_D (mM)	k_{red}/K_D (s^{-1} mM^{-1})
No ornithine	Fast	1.14±0.03	0.35±0.03	3.3±0.3
	Slow	0.073±0.004	0.19±0.04	0.38±0.08
10 mM ornithine	Fast	0.314±0.007	0.050±0.008	6±1
	Slow	0.035±0.002	0.08±0.02	0.4±0.1

IV. Discussion

This chapter reports the characterization of TheA, an NMO from *Thermocrispum agreste*. NMOs and the hydroxylation step they catalyze are characterized by their role in important non-ribosomal peptide synthesis. Most notably, members of this group have been identified as essential for pathogenesis for organisms such as *A. fumigatus*[19] and *M. tuberculosis*[40, 51] and, therefore, represent potential novel drug targets to treat microbial infections. Although the structural and chemical mechanism has been previously reported for a small number of NMOs[12, 18, 20, 24, 26, 30, 33, 36, 43], the mode of action is ambiguous and seems to vary drastically between members of the same group. Here we have investigated TheA as an enzyme model, providing valuable information that will allow for further understanding of this group of enzymes.

To achieve this goal, we cloned, heterologously expressed, and purified TheA. Purification of recombinant TheA yielded a considerable amount of pure, concentrated protein. Furthermore, the enzyme was purified with the FAD cofactor bound, as evidenced by a characteristic yellow color and the associated absorbance spectra of flavoproteins. TheA is part of the group B flavin monooxygenases, which are known to tightly bind the flavin cofactor primarily through non-covalent interactions[10]. Interestingly, the ability to purify NMOs with flavin bound and the percent incorporation can both vary between ornithine monooxygenases[18, 24, 36, 52]. Size-exclusion chromatography revealed that TheA primarily adopts octameric and pentameric quaternary structures (Table 2.1). Similarly, other NMOs are known to complex in a similar manner: PvdA acquires pentameric conformation[26] while both SidA and KtzI are reported to be tetrameric[18, 33]. Therefore,

TheA may be present in solution as tetramer structures that further interact and complex to produce the octameric state.

Results of TheA activity assays suggest that the enzyme prefers L-ornithine over L-lysine as the substrate, as previously reported[44]. Interestingly, the catalytic efficiency of oxygen consumption by TheA when using L-lysine is higher than with L-ornithine. However, none of the consumed oxygen is incorporated to form N-hydroxy lysine, as evidenced by the lack of product detection. Most likely, TheA uses the activated oxygen to produce hydrogen peroxide as an alternative mechanism in which NMOs regenerate oxidized FAD to start the mechanism again[18]. Steady state kinetic analyses also suggest that TheA prefers NADPH over NADH. Results herein indicate that the catalytic efficiency of TheA in the presence of NADPH is higher than with NADH. Furthermore, the uncoupling percentage is higher with NADH as the cofactor, thus indicating the specificity for this nicotinamide cofactor.

Interestingly, TheA seems to remain stable when incubating in temperatures up to 50 °C, but stability abruptly decreases when incubating at 60 °C. Similarly, the T_m of the enzyme in the presence of substrates is 50 °C and, according to the ThermoFAD assay, the enzyme is expected to be denatured around 60 °C. This enzymatic property is expected as *T. agreste* thrives in temperatures ranging from 28 °C to 60 °C[45]. As far as the author knows, this is the first report on the effect of temperature on the stability of an N-hydroxylating monooxygenase.

The rate of reduction of the oxidized flavin in TheA was best described using the double exponential equation that describes two distinct phases that differ in the rate of reduction and K_D. Enzyme kinetics explained by double exponential equations are thought to describe a minimal two step mechanism consisting of 1) a binding step to form a loose complex, followed by 2) isomerization to form an end tight complex[53], as observed in other enzymes such as human AKR1C2, which catalyzes a reduction step of 5α-dihydrotestosterone[54]. In the case of TheA, while the reduction of the flavin by NADPH is key for enzyme activity, the formation of an end complex between $NADP^+$ and the reduced flavoenzyme seems to be a

defined key step. Other class B NMOs are known to keep the $NADP^+$ in complex with the flavoenzyme after the reduction step. This complex fulfills a key role in the consecutive steps of the mechanism, particularly in the activation of molecular oxygen and the formation and stabilization of the C4a-hydroperoxyflavin[12-15].

Interestingly, the rate constant for flavin reduction in the presence of the substrate was slower, most notably, with a decrease of ~3.5 fold in the fast phase of the reaction. This observation sets TheA apart from other reported class B monooxygenases in which the reduction remains unchanged in the presence of the substrate[29]. This behavior has only been observed in the L-lysine monooxygenase MbsG, an enzyme that differs greatly in the mechanism with previously characterized NMOs. In this enzyme, substrate binding is thought to induce conformational changes that primes the active site to favor the hydroxylation reaction, rendering the reduction step unfavorable while enabling the activation of molecular oxygen[55]. TheA might function in a similar manner, in which the decrease of the reduction rate is caused by conformation changes upon L-ornithine binding.

TheA mechanism follows a pattern similar to other L-ornithine monooxygenases, such as *A. fumigatus* SidA[29, 56] (Figure 2.10). As determined by the steady state and presteady state kinetics, the enzyme first reduces the oxidized FAD using NADPH, following a two-step mechanism with a fast and a slow phase. The reduced flavin then will consume oxygen with a k_{cat} of 0.128 s^{-1} to form a hydroperoxyflavin intermediate, responsible of hydroxylating ornithine with a k_{cat} of 0.11 s^{-1}. The mechanism ends upon release of the N-hydroxy ornithine and $NADP^+$. The enzyme also has an alternative mechanism in which it releases H_2O_2 to regenerate oxidized FAD. The rates of hydroperoxyflavin formation and flavin oxidation have not been determined for TheA and represent the following step in the characterization of this enzyme.

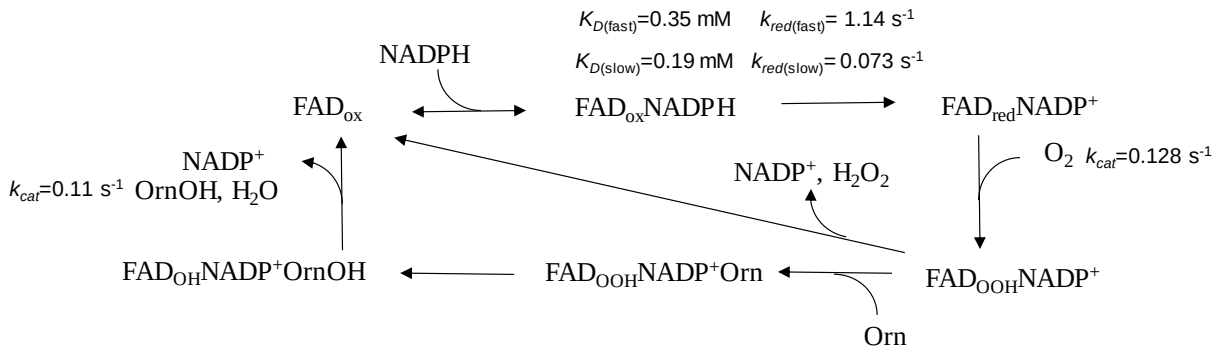

Figure 2.10 Proposed mechanism of *T. agreste* TheA.

TheA also has notable differences that set it apart from other L-ornithine monooxygenases. TheA is ~5 fold slower than SidA, as seen with the k_{cat} when following both the oxygen consumption and the product formation assays (Table 2.6). The rate limiting step in the mechanism of SidA has been determined to be the hydride transfer in the reduction step[13, 22, 56], however, this is not the same in TheA, in which the reduction step seems to be faster than both the oxygen consumption and product formation rates. To determine the rate limiting step of the mechanism of TheA, the other steps of the reaction must be characterized first, such as the rates of hydroperoxyflavin intermediate formation and flavin oxidation.

Table 2.6 Summary of the kinetic parameters of *T. agreste* TheA and *A. fumigatus* SidA.

Parameter	TheA	SidA[56]
k_{cat} O_2 consumption (s^{-1})	0.171±0.005	0.59±0.01
k_{cat} OrnOH formation (s^{-1})	0.104±0.009	0.62±0.02
$k_{red(fast)}$ (s^{-1})	1.14±0.03	0.62±0.01
$k_{red(slow)}$ (s^{-1})	0.073±0.004	0.220±0.005

CHAPTER THREE: PRODUCTION OF NADPH ANALOGUES AS PROBES TO STUDY N-HYDROXYLATING MONOOXYGENASES

I. Introduction

The mechanism of NMOs has been studied in detail, providing insights that highlight the unique characteristics of hydroxylation. The reaction starts when NADPH binds to the enzyme and reduces FAD. This step is key for flavin reactivity because it allows the formation of the oxygen adducts required for the hydroxylation of the substrates in the second half reaction[2, 10].

Previous steady state kinetic isotope effect experiments showed that the *pro*-R hydrogen at position 4 in the nicotinamide moiety of NADPH is specifically transferred to the N5 in the FAD (Figure 3.1)[13]. However, crystal structures of all NMOs reported to date show that the $NADP^+$ is not oriented facing the FAD in such way that facilitates the *pro*-R hydrogen transfer (Figure 3.2)[12, 24, 33]. Instead, the nicotinamide cofactor is in a conformation allowing for its role in stabilizing the C4a-hydroperoxyflavin. Thus, NADP(H) undergoes conformational changes after hydride transfer[22]; this is termed the sliding mechanism of NADP(H) in Class B flavin dependent monooxygenases[15, 57].

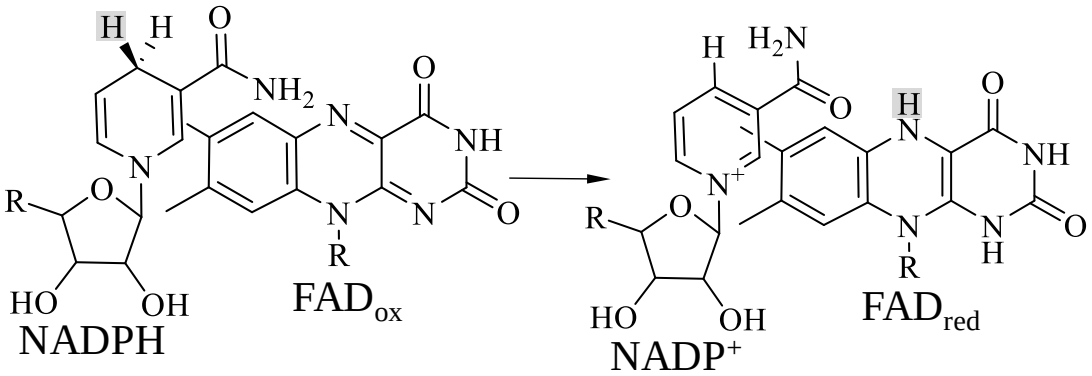

Figure 3.1 The *pro*-R hydrogen transfer in the reduction of FAD by NADPH in *A. fumigatus* SidA. The pro-R hydrogen is shaded in gray.

Even though several NMO structures have been solved at different steps of the reaction mechanism, the active site structure when NADP(H) is in a favorable position for hydride transfer has not previously been shown. This is due to challenges associated with crystallization in this conformation when using $NADP^+$ and NADPH. We, therefore, hypothesize that crystallization in the presence of NADPH analogues would capture the enzyme in this structural conformation prior to the reduction.

In this work, we produced NADPH analogues through an unspecific reduction reaction using NaB^2H_4. This process yielded [6-^{2}H]-NADPH, [2-^{2}H]-NADPH and [4-^{2}H]-NADPH. Furthermore, compound identity was confirmed by mass spectrometry and unidimensional Nuclear Magnetic Resonance (NMR).

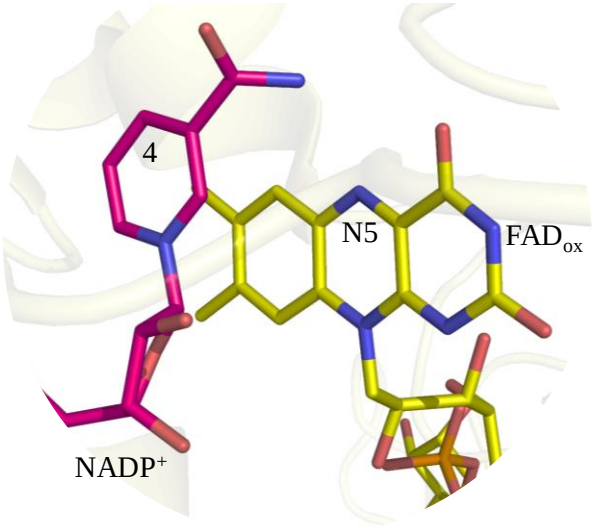

Figure 3.2 NADP+ orientation in SidA active site does not favor transfer of the pro-R hydrogen to the N5 of flavin.

II. Material and methods

3.2.1 Materials

Reagents used in this work were obtained from Fisher Scientific (Pittsburg, PA) unless otherwise stated. NADPH was purchased from Research Products International (Mt Prospect, IL) and NaB^2H_4 was purchased from Sigma Aldrich (St. Louis, MO).

3.2.2 Production of reduced deuterated $NADP^+$ analogues.

NADPH analogues were produced by the nonspecific reduction of the nicotinamide moiety[58]. Specifically, 1 mL of 40 mM $NADP^+$ in 100 mM potassium phosphate at pH 7.5 was mixed with 1 mL of 200 mM NaB^2H_4 in 20 mM potassium phosphate at pH 11. The reaction was incubated for 5 minutes on ice and then diluted with 95% ethanol in a 1:25 ratio. The ethanol-diluted mixture was incubated at -20 °C for 10 min to ensure complete precipitation. The sample was then centrifuged at 45000 g for 45 min at 4 °C. The supernatant was subsequently discarded, and the pellet was resuspended in 10 mM potassium phosphate buffer at pH 7.5. The compound mixture was aliquoted and stored at -20 °C.

3.2.3 Analytical HPLC analysis of the reduced deuterated $NADP^+$ analogues

Isolation of the reduced deuterated NADPH analogues was achieved by high-pressure liquid chromatography (HPLC) using an analytical Phenomenex Luna 5u C18 (2) reverse column (250×4.6 mm, 5 μm particle size). The compound mixture was diluted 1:200 in 10 mM potassium phosphate buffer at pH 7.5 and 50 μL of the dilution were injected. Chromatography was performed isocratically at 0.1 mL/min in 10 mM potassium phosphate, pH 7.5 buffer for 120 min. Compound separation was monitored by following the UV/vis absorption at 260 nm using a photodiode array detector.

3.2.4 Isolation of the reduced deuterated $NADP^+$ analogues:

Separation of the reduced deuterated $NADP^+$ analogues was achieved by preparative HPLC using a Phenomenex Luna 5u C18 (2) reverse column (250×21.2 mm, 5 μm particle size). Separation was performed isocratically at 4 mL/min in 10 mM potassium phosphate buffer at pH 7.5 for 120 minutes, in which 100 μL of undiluted sample was injected. Compound separation was monitored by following the UV/vis absorption at 260 nm using a photodiode array detector. Fractions exhibiting absorbance peaks were collected and stored at 4 °C.

Fractions with absorbance peaks at 344 nm and 392 nm, corresponding to [6-^{2}H]-NADPH and [2-^{2}H]-NADPH, respectively, were loaded to a 35 cc C18 Sep-Pak cartridge (Waters) and eluted with 200 mL distilled water. Samples were lyophilized and stored at -20 °C until further use.

3.2.5 Mass spectrometry of isolated peaks

Fractions corresponding to [6-^{2}H]-NADPH and [2-^{2}H]-NADPH were analyzed using an AB Sciex 4800 MALDI TOF/TOF mass spectrometer. Aliquots of 1 μL were spotted onto a MALDI target plate followed by 1 μL of matrix (4 mg/ml α-Cyano-4-hydroxycinnamic acid in 50:50 water: acetonitrile supplemented with 0.1% (v/v) trifluoroacetic acid and 10 mM ammonium chloride) and allowed to air dry. Data was collected in reflector negative ion mode with each spectrum being a sum of 1700 laser shots.

3.2.6 NMR of the isolated peaks

NMR was used to confirm the identity of the nicotinamide cofactor reduction products. Samples of [6-^{2}H]-NADPH and [2-^{2}H]-NADPH were prepared by resuspending 2 mg of purified product in 500 μL of ^2H_2O. ^{1}H-spectra were recorded on a 500 MHz Brucker Avance II instrument located in the Department of Chemistry, Virginia Tech. For each sample, 64 scans were collected.

III. Results

In this work, we synthesized NADPH analogues through a nonspecific reduction reaction using NaB^2H_4. Figure 3.3 shows a chromatogram of the products obtained from this reaction, in which five individual peaks were identified.

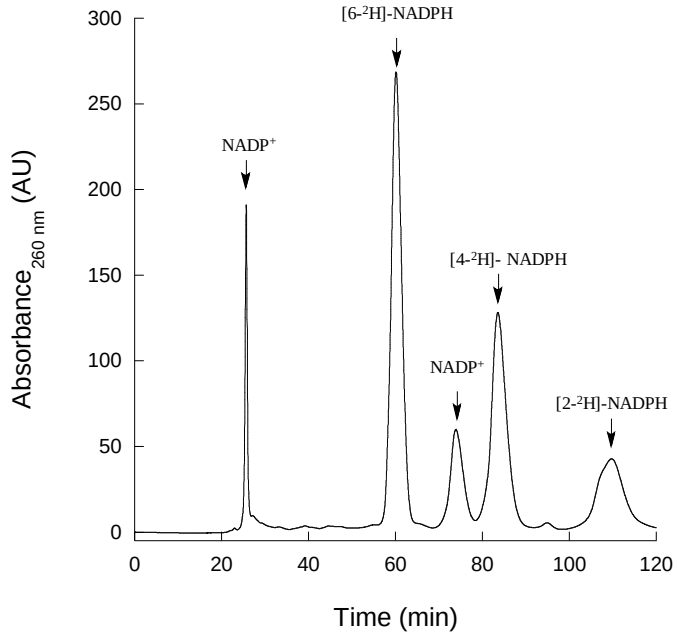

Figure 3.3 Analytical HPLC chromatogram for the mixture obtained after reduction of $NADP^+$ with NaB^2H_4. Chemical identity of the different molecules was assigned based on their absorption spectra (see main text).

The UV/Vis absorption spectrum of each peak was measured to characterize the different reduction products (Figure 3.4). All samples showed an absorption peak at 258 nm, which corresponds to absorbance of the adenine moiety. Samples with retention times of 85.0, 60.6, and 111.7 min had distinctive peaks at 338, 344, and 392 nm, respectively, corresponding to the different dihydro-nicotinamide moieties. The absorbance spectra of the NADPH molecules are dependent on the reduction site and, thus, can be used to differentiate among them[58]. Consequently, samples with maximum absorbance values at 338, 344, and 392

nm were assigned as [4-^{2}H]-NADPH, [6-^{2}H]-NADPH, and [2-^{2}H]-NADPH. Samples with retention times of 25.4 and 44.0 min did not absorb in the 300-500 nm range, indicating an absence of the reduced nicotinamide moiety; thus, they were identified as $NADP^+$. For these samples, the only absorbance peak observed at 258 nm corresponds to the overlapping absorption that results from adenine and the oxidized form of nicotinamide.

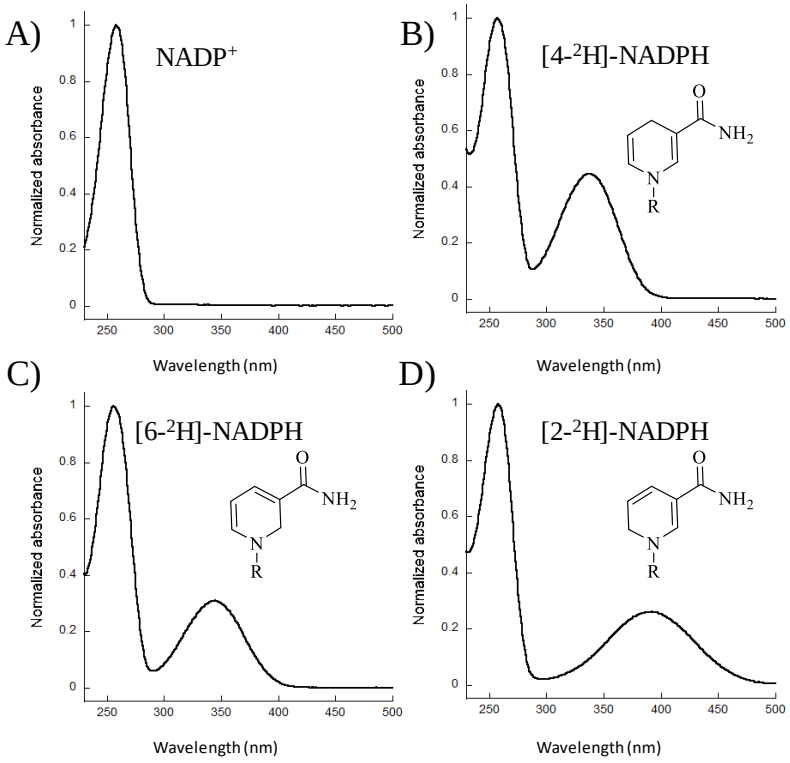

Figure 3.4 UV/Vis absorbance spectra of the purified samples. The molecule that yields the distinctive absorbance between 300 and 500 nm is shown in each spectrum. A) The samples with retention times of 25.4 and 44.0 min showed a single peak at 258 nm corresponding to the adenine moiety and oxidized nicotinamide, B) the sample with retention time of 85.0 min had a distinctive peak at 338 nm corresponding to the dihydro-nicotinamide moiety reduced at position 4, C) the sample with retention time of 60.6 min had a distinctive peak at 344 nm corresponding to the dihydro-nicotinamide moiety reduced at position 6, and D) the sample with retention time of 111.7 min had a distinctive peak at 392 nm corresponding to the dihydro-nicotinamide moiety reduced at position 2.

The samples assigned as [6-^{2}H]-NADPH and [2-^{2}H]-NADPH based on their absorbance spectra were further characterized through MALDI TOF/TOF mass spectrometry. The mass spectra of [6-^{2}H]-NADPH and [2-^{2}H]-NADPH (Figure 3.5.B and Figure 3.5.C, respectively) displayed a similar fragmentation pattern to that of commercially available NADPH, which was used as control (Figure 3.5.A). As expected for deuterated products, the mass-to-charge ratio (m/z) of the molecular ions for [6-^{2}H]-NADPH and [2-^{2}H]-NADPH were one unit higher than that of the NADPH control, with values of 745.1 as opposed to 744.1 (Figure 3.6).

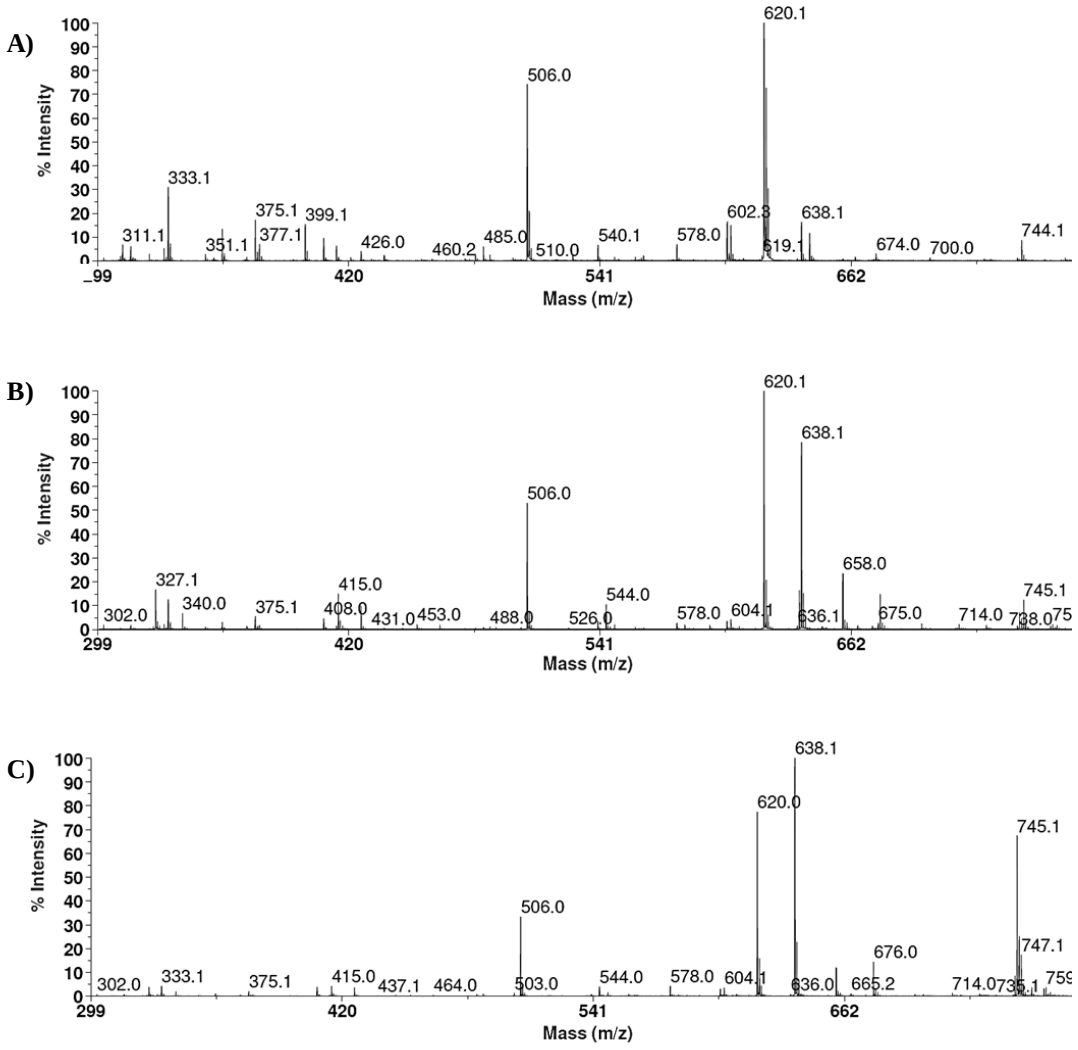

Figure 3.5 Mass spectra of deuterated NADPH analogues. A) non-deuterated NADPH, B) [6-^{2}H]-NADPH, and C) [2-^{2}H]-NADPH.

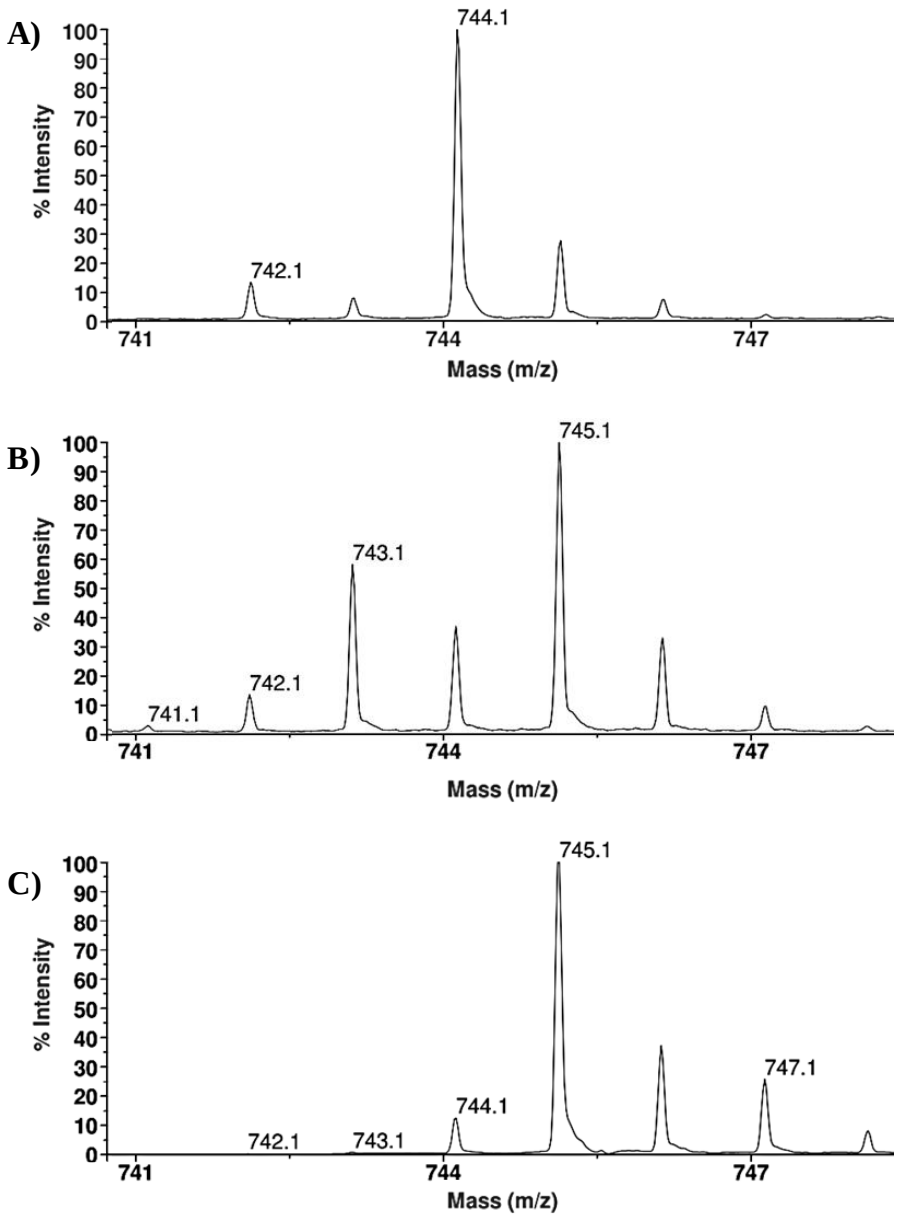

Figure 3.6 Zoomed in mass spectra of deuterated NADPH analogues. A) non-deuterated NADPH, B) [6-^{2}H]-NADPH, and C) [2-^{2}H]-NADPH.

One-dimensional (1D) ^{1}H-NMR spectra were obtained for the isolated [6-H]-NADP and [2-H]-NADP in order to further confirm their chemical identity. The spectra collected for [6-H]-NADP displays peaks at positions expected for the hydrogens in the reduced nicotinamide moiety (Figure 3.7). Specifically, the

peaks observed between 3.65 and 3.50 ppm are attributed to the protons located at the C6 position. In contrast, poor signal-to-noise ratio obtained in the [2-H]-NADP spectra hindered its comparison with that of [6-H]-NADP. However, we were able to observe peaks that correspond to the hydrogens located at the C2 position, which display chemical shifts in the 3.65-3.50 ppm range.

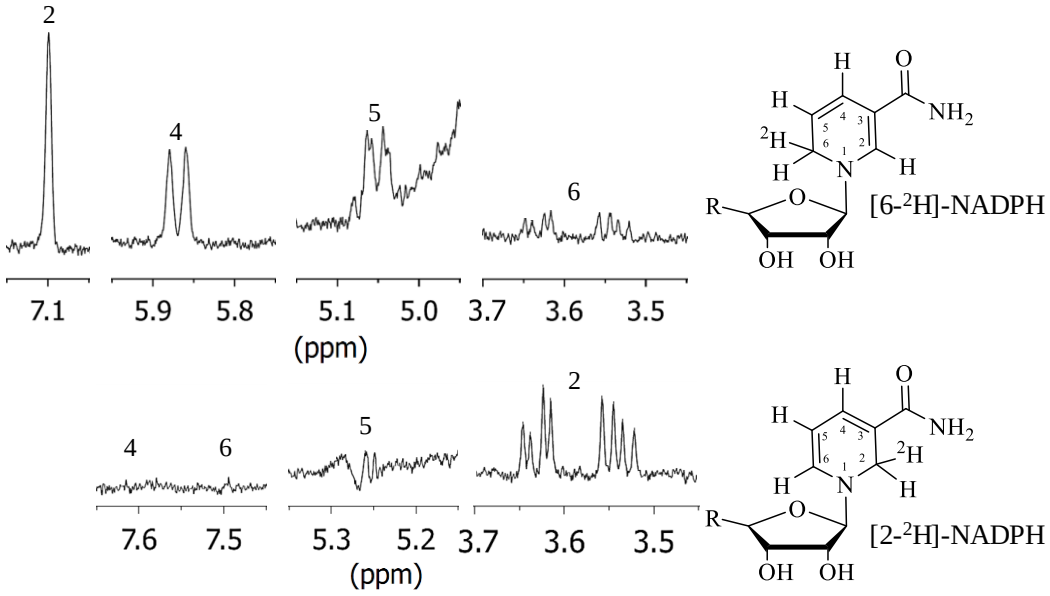

Figure 3.7 NMR identification of A) [6-^{2}H]-NADPH and B) [2-^{2}H]-NADPH.

IV. Discussion

Herein, we report the unspecific reduction of $NADP^+$ by NaB^2H_4. Through this reaction, we were able to produce and purify [4-^{2}H]-NADPH, [6-^{2}H]-NADPH, and [2-^{2}H]-NADPH. The reduction of the nicotinamide moiety with $NaBH_4$[59-62] and purification of the associated products[58] has only been reported when NAD^+ was used as the substrate. Thus, this work presents the first report detailing the unspecific reduction of $NADP^+$ through this reaction. The absorbance spectra were used to determine product identity based on previously reported absorbance of the reduced nicotinamide moieties[58].

Furthermore, with NaB^2H_4 as the reducing agent, the resulting products are expected to have deuterium in the C4 that is reduced. Mass spectra of fractions containing [6-^{2}H]-NADPH and [2-^{2}H]-NADPH have a distinct peak at 745.1 m/z that corresponds to the parent molecule. When comparing to the 744.1 m/z peak of the undeuterated NADPH control parent molecule, there is a shift of +1. This confirms deuterium incorporation via reduction by NaB^2H_4.

Further characterization by one-dimensional (1D) ^{1}H-NMR confirmed the reduction site of [6-^{2}H]-NADPH. It is important to note that, since this is an unspecific reaction, deuterium incorporation will occur indiscriminately in either the pro-R or pro-S position. Thus, although there is deuterium incorporation, the presence of both possible conformations will produce a signal for the two hydrogens at position 6, as observed in the chemical shifts in the 3.65–3.50 ppm range. Altogether, combined results of the UV/Vis absorbance spectra, mass spectrometry, and ^{1}H-NMR analyses confirm the identity of [6-^{2}H]-NADPH.

Although the ^{1}H-NMR of the [2-^{2}H]-NADPH did not show all expected chemical shifts due to poor signal-to-noise ratio, the presence of chemical shifts in the 3.65–3.50 ppm range, as well as both the UV/Vis absorbance and mass spectra results, confirmed identity of [2-^{2}H]-NADPH. Further NMR experiments should be pursued to fully characterize [2-^{2}H]-NADPH and the other isolated fractions.

It is worth noting that there are other methods that can also be pursued to produce NADPH analogues, such as the enzymatic reduction of $NADP^+$ that yields stereospecific addition of hydrogen at position 4[63]. Other reducing agents, such as $NaBH_3CN$[64] and NaS_2O_4[58], reduce $NADP^+$ and favor the production of [4-DH]-NADP. However, $NaBH_4$ is the only reducing agent reported to produce all analogues in the same reaction[58]. Specific chemical reactions, such as that reported here, provide access to analogues that may otherwise be unobtainable through enzymatic reactions and other conventional methods.

CHAPTER FOUR: CONCLUDING REMARKS

I. Enzymatic characterization of TheA

Herein we present the characterization of *T. agreste* TheA. The enzyme mechanism was studied using diverse techniques such as product formation, oxygen consumption, and stopped flow spectrophotometry assays. We determined the catalytic rates, substrate binding affinities, and coenzyme specificities. Results revealed that TheA prefers L-ornithine and NADPH as the substrate and cosubstrate of the reaction. Furthermore, results indicate that TheA is thermally stable in temperatures up to 50 °C. The presteady state kinetic analysis revealed that the reduction reaction occurs in a two-step mechanism, suggesting isomerization of the active site to form an end tight complex of $NADP^+$ and reduced FAD. Finally, we discovered that binding of L-ornithine inhibits the reduction step, suggesting that substrate binding induces conformational changes that are not favorable for FAD reduction. Although TheA follows a mechanism similar to other L-ornithine monooxygenases such as SidA, this key enzyme feature has not been previously reported in this enzyme group: the novel TheA enzyme mechanism reported here sets this enzyme apart from previously reported members of this group.

Further characterization of TheA must be performed to further understand the nuances of its mechanism. The rapid reaction kinetics following the oxidative half reaction will provide further insights into the mechanism of hydroperoxyflavin formation and regeneration of oxidized flavin. Given the unique mechanism of TheA, studying the oxidative half reaction in the presence of L-ornithine will be of particular interest. Additionally, future work should focus on the structure determination of TheA to describe the structural features of TheA that may be responsible for its mechanism diverging from other NMOs. The combined results of this study will improve the general knowledge and understanding of flavoenzymes, ornithine monooxygenases, and their associated mechanisms.

II. Production of NADPH analogues as probes to study N-hydroxylating monooxygenases

In this work, we produced NADPH analogues through an unspecific reduction reaction using NaB^2H_4. This process yielded [6-^{2}H]-NADP, [2-^{2}H]-NADP, and [4-^{2}H]-NADPH. Furthermore, compound identity was confirmed by mass spectrometry and unidimensional nuclear magnetic resonance (NMR). This work presents the first report detailing the unspecific reduction of $NADP^+$ through this reaction.

The use of NADPH analogues for probing the mechanism of flavin reduction TheA will serve as the foundation for future studies of NMOs employing NADPH analogues. Although we were able to successfully produce and purify NADPH analogues and confirmed the identity of [6-^{2}H]-NADPH and [2-^{2}H]-NADPH, further study is required to identify the other reaction products.

These products will be used to capture NMOs in the conformation that facilitates the reduction of FAD, as this has not been previously reported. TheA and SidA will serve as model enzymes; SidA is of particular interest, due to the thorough characterization of its mechanism as well as the establishment of techniques and conditions for reliable and successful growth of crystals. Additionally, the behavior of L-ornithine NMOs upon addition of these analogues will be studied using isothermal titration calorimetry, steady state kinetics, and rapid reaction kinetics.

REFERENCE LIST

[1] Joosten, V., and van Berkel, W. J. H. (2007) Flavoenzymes, *Current Opinion in Chemical Biology 11*, 195-202.

[2] Walsh, C. T., and Wencewicz, T. A. (2013) Flavoenzymes: Versatile Catalysts in Biosynthetic Pathways, *Natural product reports 30*.

[3] Walsh, C. (1980) Flavin coenzymes: at the crossroads of biological redox chemistry, *Accounts of Chemical Research 13*, 148-155.

[4] Macheroux, P., Kappes, B., and Ealick, S. E. (2011) Flavogenomics a genomic and structural view of flavin-dependent proteins, *The FEBS Journal 278*, 2625-2634.

[5] Ghisla, S., and Massey, V. (1989) Mechanisms of flavoprotein-catalyzed reactions, *European Journal of Biochemistry 181*, 1-17.

[6] Porter, D. J. T., Voet, J. G., and Bright, H. J. (1973) Direct Evidence for Carbanions and Covalent N5-Flavin-Carbanion Adducts as Catalytic Intermediates in the Oxidation of Nitroethane by d-Amino Acid Oxidase, *Journal of Biological Chemistry 248*, 4400-4416.

[7] Thorpe, C., and Williams, C. H., Jr. (1976) Spectral evidence for a flavin adduct in a monoalkylated derivative of pig heart lipoamide dehydrogenase, *J Biol Chem 251*, 7726-7728.

[8] Massey, V. (1994) Activation of molecular oxygen by flavins and flavoproteins, *J Biol Chem 269*, 22459-22462.

[9] Huijbers, M. M. E., Montersino, S., Westphal, A. H., Tischler, D., and van Berkel, W. J. H. (2014) Flavin dependent monooxygenases, *Archives of Biochemistry and Biophysics 544*, 2-17.

[10] van Berkel, W. J. H., Kamerbeek, N. M., and Fraaije, M. W. (2006) Flavoprotein monooxygenases, a diverse class of oxidative biocatalysts, *Journal of Biotechnology 124*, 670-689.

[11] Ballou, D., and Entsch, B. (2013) The reaction mechanisms of groups A and B flavoprotein monooxygenases.

[12] Franceschini, S., Fedkenheuer, M., Vogelaar, N. J., Robinson, H. H., Sobrado, P., and Mattevi, A. (2012) Structural insight into the mechanism of oxygen activation and substrate selectivity of flavin-dependent N-hydroxylating monooxygenases, *Biochemistry 51*, 7043-7045.

[13] Romero, E., Fedkenheuer, M., Chocklett, S. W., Qi, J., Oppenheimer, M., and Sobrado, P. (2012) Dual role of NADP(H) in the reaction of a flavin dependent N-hydroxylating monooxygenase, *Biochimica et Biophysica Acta (BBA) - Proteins and Proteomics 1824*, 850-857.

[14] Orru, R., Pazmiño, D. E. T., Fraaije, M. W., and Mattevi, A. (2010) Joint Functions of Protein Residues and NADP(H) in Oxygen Activation by Flavin-containing Monooxygenase, *The Journal of Biological Chemistry 285*, 35021-35028.

[15] Orru, R., Dudek, H. M., Martinoli, C., Torres Pazmino, D. E., Royant, A., Weik, M., Fraaije, M. W., and Mattevi, A. (2011) Snapshots of enzymatic baeyer-villiger catalysis: oxygen activation and intermediate stabilization, *Journal of Biological Chemistry*.

[16] Riebel, A., Dudek, H. M., de Gonzalo, G., Stepniak, P., Rychlewski, L., and Fraaije, M. W. (2012) Expanding the set of rhodococcal Baeyer–Villiger monooxygenases by high-throughput cloning, expression and substrate screening, *Applied Microbiology and Biotechnology 95*, 1479-1489.

[17] Zhao, Y., Christensen, S. K., Fankhauser, C., Cashman, J. R., Cohen, J. D., Weigel, D., and Chory, J. (2001) A Role for Flavin Monooxygenase-Like Enzymes in Auxin Biosynthesis, *Science 291*, 306-309.
[18] Chocklett, S. W., and Sobrado, P. (2010) Aspergillus fumigatus SidA Is a Highly Specific Ornithine Hydroxylase with Bound Flavin Cofactor, *Biochemistry 49*, 6777-6783.
[19] Hissen, A. H. T., Wan, A. N. C., Warwas, M. L., Pinto, L. J., and Moore, M. M. (2005) The Aspergillus fumigatus Siderophore Biosynthetic Gene sidA, Encoding l-Ornithine N5-Oxygenase, Is Required for Virulence, *Infection and Immunity 73*, 5493-5503.
[20] Robinson, R., Badieyan, S., and Sobrado, P. (2013) C4a-Hydroperoxyflavin Formation in N-Hydroxylating Flavin Monooxygenases Is Mediated by the 2′-OH of the Nicotinamide Ribose of NADP+, *Biochemistry 52*, 9089-9091.
[21] Robinson, R., Franceschini, S., Fedkenheuer, M., Rodriguez, P. J., Ellerbrock, J., Romero, E., Echandi, M. P., Martin del Campo, J. S., and Sobrado, P. (2014) Arg279 is the key regulator of coenzyme selectivity in the flavin-dependent ornithine monooxygenase SidA, *Biochimica et Biophysica Acta (BBA) - Proteins and Proteomics 1844*, 778-784.
[22] Shirey, C., Badieyan, S., and Sobrado, P. (2013) Role of Ser-257 in the Sliding Mechanism of NADP(H) in the Reaction Catalyzed by the Aspergillus fumigatus Flavin-dependent Ornithine N5-Monooxygenase SidA, *Journal of Biological Chemistry 288*, 32440-32448.
[23] Meneely, K. M., and Lamb, A. L. (2007) Biochemical Characterization of a Flavin Adenine Dinculeotide-Dependent Monooxygenase, Ornithine Hydroxylase from Pseudomonas aeruginosa, Suggests a Novel Reaction Mechanism, *Biochemistry 46*, 11930-11937.
[24] Olucha, J., Meneely, K. M., Chilton, A. S., and Lamb, A. L. (2011) Two structures of an N-hydroxylating flavoprotein monooxygenase: ornithine hydroxylase from Pseudomonas aeruginosa, *J Biol Chem 286*, 31789-31798.
[25] Visca, P., Ciervo, A., and Orsi, N. (1994) Cloning and nucleotide sequence of the pvdA gene encoding the pyoverdin biosynthetic enzyme L-ornithine N5-oxygenase in Pseudomonas aeruginosa, *J Bacteriol 176*, 1128-1140.
[26] Ge, L., and Seah, S. Y. K. (2006) Heterologous Expression, Purification, and Characterization of an l-Ornithine N5-Hydroxylase Involved in Pyoverdine Siderophore Biosynthesis in Pseudomonas aeruginosa, *Journal of Bacteriology 188*, 7205-7210.
[27] Kumar, S., Stecher, G., and Tamura, K. (2016) MEGA7: Molecular Evolutionary Genetics Analysis Version 7.0 for Bigger Datasets, *Molecular Biology and Evolution 33*, 1870-1874.
[28] Romero, E., Avila, D., and Sobrado, P. (2013) Effect of pH on the Reductive and Oxidative Half-reactions of Aspergillus fumigatus Siderophore A.
[29] Mayfield, J. A., Frederick, R. E., Streit, B. R., Wencewicz, T. A., Ballou, D. P., and DuBois, J. L. (2010) Comprehensive Spectroscopic, Steady State, and Transient Kinetic Studies of a Representative Siderophore-associated Flavin Monooxygenase, *Journal of Biological Chemistry 285*, 30375-30388.
[30] Badieyan, S., Bach, R. D., and Sobrado, P. (2015) Mechanism of N-Hydroxylation Catalyzed by Flavin-Dependent Monooxygenases, *The Journal of Organic Chemistry 80*, 2139-2147.
[31] Binda, C., Robinson, R. M., Martin Del Campo, J. S., Keul, N. D., Rodriguez, P. J., Robinson, H. H., Mattevi, A., and Sobrado, P. (2015) An unprecedented NADPH domain conformation in lysine monooxygenase NbtG provides insights into uncoupling of oxygen consumption from substrate hydroxylation, *J Biol Chem 290*, 12676-12688.

[32] Salomone-Stagni, M., Bartho, J. D., Polsinelli, I., Bellini, D., Walsh, M. A., Demitri, N., and Benini, S. (2018) A complete structural characterization of the desferrioxamine E biosynthetic pathway from the fire blight pathogen Erwinia amylovora, *Journal of structural biology*.

[33] Setser, J. W., Heemstra, J. R., Walsh, C. T., and Drennan, C. L. (2014) Crystallographic Evidence of Drastic Conformational Changes in the Active Site of a Flavin-Dependent N-Hydroxylase, *Biochemistry 53*, 6063-6077.

[34] Stehr, M., Diekmann, H., Smau, L., Seth, O., Ghisla, S., Singh, M., and Macheroux, P. (1998) A hydrophobic sequence motif common to N-hydroxylating enzymes, *Trends Biochem Sci 23*, 56-57.

[35] Olucha, J., and Lamb, A. L. (2011) Mechanistic and structural studies of the N-hydroxylating flavoprotein monooxygenases, *Bioorg Chem 39*, 171-177.

[36] Neumann, C. S., Jiang, W., Heemstra, J. R., Gontang, E. A., Kolter, R., and Walsh, C. T. (2012) Biosynthesis of Piperazic Acid via N5-Hydroxy-Ornithine in Kutzneria spp. 744, *ChemBioChem 13*, 972-976.

[37] Neilands, J. B. (1995) Siderophores: Structure and Function of Microbial Iron Transport Compounds, *Journal of Biological Chemistry 270*, 26723-26726.

[38] Schrettl, M., Bignell, E., Kragl, C., Joechl, C., Rogers, T., Arst, H. N., Haynes, K., and Haas, H. (2004) Siderophore Biosynthesis But Not Reductive Iron Assimilation Is Essential for Aspergillus fumigatus Virulence, *The Journal of Experimental Medicine 200*, 1213-1219.

[39] Lamont, I. L., Beare, P. A., Ochsner, U., Vasil, A. I., and Vasil, M. L. (2002) Siderophore-mediated signaling regulates virulence factor production in Pseudomonas aeruginosa, *Proceedings of the National Academy of Sciences of the United States of America 99*, 7072-7077.

[40] Wells, R. M., Jones, C. M., Xi, Z., Speer, A., Danilchanka, O., Doornbos, K. S., Sun, P., Wu, F., Tian, C., and Niederweis, M. (2013) Discovery of a Siderophore Export System Essential for Virulence of Mycobacterium tuberculosis, *PLOS Pathogens 9*, e1003120.

[41] Martín del Campo, J. S., Vogelaar, N., Tolani, K., Kizjakina, K., Harich, K., and Sobrado, P. (2016) Inhibition of the Flavin-Dependent Monooxygenase Siderophore A (SidA) Blocks Siderophore Biosynthesis and Aspergillus fumigatus Growth, *ACS Chemical Biology 11*, 3035-3042.

[42] Kodani, S., Komaki, H., Suzuki, M., Hemmi, H., and Ohnishi-Kameyama, M. (2015) Isolation and structure determination of new siderophore albachelin from Amycolatopsis alba, *BioMetals 28*, 381-389.

[43] Frederick, R. E., Mayfield, J. A., and DuBois, J. L. (2011) Regulated O2 Activation in Flavin-Dependent Monooxygenases, *Journal of the American Chemical Society 133*, 12338-12341.

[44] Heine, T., Mehnert, M., Schwabe, R., and Tischler, D. (2017) *Thermochelin, a Hydroxamate Siderophore from Thermocrispum agreste DSM 44070*, Vol. 262.

[45] Korn-Wendisch, F., Rainey, F., Kroppenstedt, R. M., Kempf, A., Majazza, A., Kutzner, H. J., and Stackebrandt, E. (1995) Thermocrispum gen. nov., a New Genus of the Order Actinomycetales, and Description of Thermocrispum municipale sp. nov. and Thermocrispum agreste sp. nov, *International Journal of Systematic and Evolutionary Microbiology 45*, 67-77.

[46] Li, W., Cowley, A., Uludag, M., Gur, T., McWilliam, H., Squizzato, S., Park, Y. M., Buso, N., and Lopez, R. (2015) The EMBL-EBI bioinformatics web and programmatic tools framework, *Nucleic Acids Research 43*, W580-W584.
[47] Fox, B. G., and Blommel, P. G. (2001) Autoinduction of Protein Expression, In *Current Protocols in Protein Science*, John Wiley & Sons, Inc.
[48] Csaky, T. (1948) On the estimation of bound hydroxylamine in biological materials., *Acta chem. Scand*, 450-454.
[49] Forneris, F., Orru, R., Bonivento, D., Chiarelli, L. R., and Mattevi, A. (2009) ThermoFAD, a Thermofluor®-adapted flavin ad hoc detection system for protein folding and ligand binding, *The FEBS Journal 276*, 2833-2840.
[50] Romero, E., Robinson, R., and Sobrado, P. (2012) Monitoring the Reductive and Oxidative Half-Reactions of a Flavin-Dependent Monooxygenase using Stopped-Flow Spectrophotometry, *Journal of Visualized Experiments*, e3803.
[51] De Voss, J. J., Rutter, K., Schroeder, B. G., Su, H., Zhu, Y., and Barry, C. E. (2000) The salicylate-derived mycobactin siderophores of Mycobacterium tuberculosis are essential for growth in macrophages, *Proceedings of the National Academy of Sciences 97*, 1252-1257.
[52] Bufkin, K., and Sobrado, P. (2017) Characterization of the Ornithine Hydroxylation Step in Albachelin Biosynthesis, *Molecules 22*, 1652.
[53] Huddleston, J. P., Schroeder, G. K., Johnson, K. A., and Whitman, C. P. (2012) A Pre-Steady State Kinetic Analysis of the αY60W mutant of trans-3-Chloroacrylic Acid Dehalogenase: Implications for the Mechanism of the Wild-type Enzyme, *Biochemistry 51*, 9420-9435.
[54] Jin, Y., and Penning, T. M. (2006) Multiple steps determine the overall rate of the reduction of 5α-dihydrotestosterone catalyzed by human type 3 3α-hydroxysteroid dehydrogenase (AKR1C2): Implications for the Elimination of Androgens, *Biochemistry 45*, 13054-13063.
[55] Robinson, R. M., Rodriguez, P. J., and Sobrado, P. (2014) Mechanistic studies on the flavin-dependent N6-lysine monooxygenase MbsG reveal an unusual control for catalysis, *Archives of Biochemistry and Biophysics 550-551*, 58-66.
[56] Robinson, R., Qureshi, I. A., Klancher, C. A., Rodriguez, P. J., Tanner, J. J., and Sobrado, P. (2015) Contribution to catalysis of ornithine binding residues in ornithine N5-monooxygenase, *Arch Biochem Biophys 585*, 25-31.
[57] Mirza, I. A., Yachnin, B. J., Wang, S., Grosse, S., Bergeron, H., Imura, A., Iwaki, H., Hasegawa, Y., Lau, P. C. K., and Berghuis, A. M. (2009) Crystal Structures of Cyclohexanone Monooxygenase Reveal Complex Domain Movements and a Sliding Cofactor, *Journal of the American Chemical Society 131*, 8848-8854.
[58] Beaupre, B. A., Hoag, M. R., Roman, J., Försterling, F. H., and Moran, G. R. (2015) Metabolic Function for Human Renalase: Oxidation of Isomeric Forms of β-NAD(P)H that Are Inhibitory to Primary Metabolism, *Biochemistry 54*, 795-806.
[59] Mathews, M. B., and Conn, E. E. (1953) The Reaction of Diphosphopyridine Nucleotide with Sodium Borohydride—A Correction and Extension, *Journal of the American Chemical Society 75*, 5428-5430.
[60] Godtfredsen, S. E., Ottesen, M., and Andersen, N. R. (1979) On the mode of formation of 1,6-dihydro-NAD in NADH preparations, *Carlsberg Research Communications 44*, 65.

[61] Godtfredsen, S. E., and Ottesen, M. (1978) 1,6-dihydro-NAD as an humidity-induced lactate dehydrogenase inhibitor in NADH preparations, *Carlsberg Research Communications 43*, 171-175.
[62] Chaykin, S., and Meissner, L. (1964) The borohydride reduction products of DPN, *Biochemical and Biophysical Research Communications 14*, 233-240.
[63] Ottolina, G., Riva, S., Carrea, G., Danieli, B., and Buckmann, A. F. (1989) Enzymatic synthesis of [4R-2H]NAD(P)H and [4S-2H]NAD(P)H and determination of the stereospecificity of 7α- and 12α-hydroxysteroid dehydrogenase, *Biochimica et Biophysica Acta (BBA) - Protein Structure and Molecular Enzymology 998*, 173-178.
[64] Avigad, G. (1979) Reduction of nicotinamide adenine dinucleotides by sodium cyanoborohydride, *Biochimica et Biophysica Acta (BBA) - Enzymology 571*, 171-174.